University of Tennessee, Knoxville

TRACE: Tennessee Research and Creative Exchange

Masters Theses

Graduate School

5-1998

# Vibrational analysis of growth hormone modulated healing of a canine radial partial ostectomy

Joseph P. Weigel

Follow this and additional works at: https://trace.tennessee.edu/utk_gradthes

## Recommended Citation

Weigel, Joseph P., "Vibrational analysis of growth hormone modulated healing of a canine radial partial ostectomy. " Master's Thesis, University of Tennessee, 1998.
https://trace.tennessee.edu/utk_gradthes/10428

This Thesis is brought to you for free and open access by the Graduate School at TRACE: Tennessee Research and Creative Exchange. It has been accepted for inclusion in Masters Theses by an authorized administrator of TRACE: Tennessee Research and Creative Exchange. For more information, please contact trace@utk.edu.

To the Graduate Council:

I am submitting herewith a thesis written by Joseph P. Weigel entitled "Vibrational analysis of growth hormone modulated healing of a canine radial partial ostectomy." I have examined the final electronic copy of this thesis for form and content and recommend that it be accepted in partial fulfillment of the requirements for the degree of Master of Science, with a major in Engineering Science.

John H. Forrester, Major Professor

We have read this thesis and recommend its acceptance:

Jack F. Wasserman, Richard J. Jendrucko

Accepted for the Council:
Carolyn R. Hodges

Vice Provost and Dean of the Graduate School

(Original signatures are on file with official student records.)

To the Graduate Council

I am submitting herewith a thesis written by Joseph Paul Weigel entitled "Vibrational Analysis of Growth Hormone Modulated Healing of a Canine Radial Partial Ostectomy." I have examined the final copy of this thesis for form and content and recommend that it be accepted in partial fulfillment of the requirements for the degree of Master of Science, with a major in Engineering Science.

John H. Forrester, PhD, Major Professor

We have read this thesis and
recommend its acceptance:

Jack F. Wasserman, PhD

Richard J. Jendrucko, PhD

Accepted for the Council:

Associate Vice Chancellor and
Dean of The Graduate School

# VIBRATIONAL ANALYSIS OF GROWTH HORMONE MODULATED HEALING OF A CANINE RADIAL PARTIAL OSTECTOMY

A Thesis

Presented for the

Master of Science

Degree

The University of Tennessee, Knoxville

Joseph Paul Weigel, DVM

May 1998

Copyright © Joseph Paul Weigel, 1998

All rights reserved

# DEDICATION

This thesis is dedicated to my parents

**Mr. and Mrs. Paul Weigel**

Their unwavering support throughout my life has been a major factor in the success I have experienced. It is to them, their patience, their love and their perseverance that I dedicate this work.

# ACKNOWLEDGMENTS

With any accomplishment in my life there are always those who have played an active or supportive role. I am indebted to all these listed here for their contribution.

I am indebted to **Dr. Jack Wasserman** who was the key person to initiate my program. His inspiration, knowledge, and patience lifted my spirits during those periods when progress seemed so slow.

I am deeply appreciative of **Dr. Jack Forrester** who graciously accepted the role as my major professor when professional commitments prevented Dr. Wasserman from continuing in that capacity. Without his advocacy and personal sacrifice, I would not have been able to reach this point.

I am thankful to **Dr. Rich Jendrucko** and **Dr. Judy Cezeaux** who were willing to serve on my committee. Without their support, this program could not have been brought to conclusion.

I am also thankful to all the engineering and mathematics faculty that I had the privilege to associate with over these past years. Their talents and interest was an inspiration to me.

Special thanks are in order to **Mr. Logan Mullinix** who provided necessary technical assistance. Also, to **Mr. Ken Thomas** and his assistants who manufactured custom testing apparatus for this project, I owe appreciation. I am grateful to **Ms Becky Greene** for the preparation of the manuscript.

I owe a debt of gratitude to **Dr. Darryl Millis** who willingly allowed vibrational testing to be part of his overall research in fracture healing. His technical advice and contribution to the statistical analysis was greatly appreciated.

I also thank my department head, **Dr. D. J. Krahwinkel**, who was patient with my effort.

Finally on a personal level, I am deeply thankful to my wife **Susan Weigel**, who remained patient and supportive especially through the highs and lows of the program and the long weekends and nights spent away from the family. I thank my children **Stephen**, **Christopher**, **Melissa**, and **Regina** for their patience and support. Ultimately I am thankful to my **Lord and Savior Jesus Christ** for creating a fascinating world and giving me certain abilities and interest in exploring His world. To Him belongs the credit.

# ABSTRACT

Sixteen adult Beagle dogs had a single partial radial ostectomy providing a 3 mm gap in the middle of the bone. The dogs were divided into 4 groups based on the duration of treatment with growth hormone, somatotropin. Group 0, the control group, received no somatotropin; group 3 received 3 weeks of treatment; group 6 received 6 weeks of treatment and group 12 received 12 weeks of treatment. At the end of the 12 week healing period, the dogs were humanely euthanatized. The healing radius and the normal contralateral radius were excised and tested by vibration and three point bending. Vibration testing included impact testing, and the development of a transfer function and frequency response curve. From the response curve, the natural frequency of the first bending mode was determined. Also the percent of damping was calculated. As the ostectomy healed and increased in stability, the natural frequency increased. The natural frequencies were significantly different with respect to the structural integrity and stability of the bones. Also the natural frequencies positively correlated with the results obtained with three point bending. Calculated damping values were not significantly different and were negatively correlated with the bending tests.

# TABLE OF CONTENTS


CHAPTER PAGE

I. INTRODUCTION ..... 1
- Problem Statement
- Research Applications
- Clinical Applications
- Hypotheses

II. REVIEW OF THE LITERATURE ..... 5
- Growth Hormone and Fracture Healing
- Evaluation of Fracture Healing
- Vibrational Analysis of Fracture Healing

III. THEORETICAL BASIS ..... 15
- Beam Analysis
  - Curvature and Deflection
  - Curvature and Flexural Rigidity
  - Deflection of Cantilever Beam
- Vibrational Analysis
  - Natural Frequency and Flexural Rigidity
  - Damping
  - Frequency Response Function
  - Fourier Analysis
- Summary

IV. MATERIALS AND METHODS ..... 38
- Design
- Data Collection and Processing
  - Transduction
  - Force Transducer
  - Accelerometer
  - Preprocessing (Amplification)
  - Postprocessing (Analyzer Function)
    - Analog to Digital Conversion
    - Analyzer Protocol
  - Measure
  - Window
  - Average
  - Frequency
  - Trigger

Input
Data Analysis
Frequency Response Function (Transfer Function)
Power Spectrums
Coherence
Real and Imaginary Plots
Damping
Statistical Analysis

V. RESULTS ..... 57
Natural Frequency
Damping

VI. DISCUSSION ..... 62
Bone Healing
Growth Hormone Effects
Nonunion Fracture Model
Callus Nonhomogeneity and Geometry
Natural Frequency
Trial Samples
Steel Bar
Trial Intact Dry Bone
Trial Taped Dry Bone
Experimental Samples
Intact Bone Specimens
Ostectomized Bones
Control Group
Group 3
Group 6
Group 12
Damping
Impact Testing

VII. CONCLUSION ..... 90

VIII. RECOMMENDATIONS FOR FUTURE STUDY ..... 91

REFERENCES ..... 92

BIBLIOGRAPHY ..... 93

VITA ..... 99

# LIST OF FIGURES

FIGURE PAGE

4-1. Fixturing apparatus for stabilizing bone samples for impact testing . . . . . 40

4-2. Schematic of the point of impact and the position of the accelerometer . . . . . 40

4-3. Schematic for data acquisition and processing . . . . . 41

4-4. Analyzer protocol for impact testing of all bone samples . . . . . 46

5-1. The natural frequency showed a gradual increase in value linearly corresponding to the increasing length of treatment with somatotropin . . . . . 60

5-2. Damping as expected is high in the control group, but because of wide variance within this group there were no significant differences between the groups . . . . . 61

6-1. Frequency response curve and coherence for the impact test of a rectangular steel bar . . . . . 68

6-2. Input power spectrum 1 and output power spectrum 2 for the rectangular steel bar . . . . . 71

6-3. Real and imaginary coefficients for the impact test of the rectangular steel bar . . . . . 71

6-4. Between 0 and approximately 500 Hz, there are no resonant frequency peaks in this frequency response curve for the steel bar . . . . . 72

6-5. A severe drop in coherence is associated with this frequency response curve for the trial intact dry bone specimen . . . . . 73

6-6. Power spectrum 2 shows four small peaks in addition to the single large output peak . . . . . 74

6-7. In these plots from the trial intact dry bone specimen, the maximum imaginary coefficient value corresponds with a near zero value for the real coefficient . . . . . 75

6-8. In this frequency response curve of the trial taped bone specimen, multiple smaller peaks are present throughout the frequency range (0 - 1 kHz) . . . . . 76

6-9. In the trial taped dry bone specimen, both power spectral curves show additional peaks indicating the presence of additional input and output energies . . . . . 77

6-10. The resonant frequency peaks of this intact experimental sample from the control group shows a notch with a severe drop in coherence . . . . . 78

6-11. An example of an intact specimen with a clean resonant peak and good coherence . . . . . 79

6-12. The frequency response curve from this ostectomized control specimen clearly demonstrates multiple resonant peaks throughout the frequency range (0 - 1 kHz) . . . . . 81

6-13. The power spectral curves from this ostectomized control specimen display the additional input and output energies frequently seen in the severely unstable bone specimens . . . . . 82

6-14. The frequency response curve from a 12 week treated ostectomy specimen with a stable callus displays the notched peak seen in some of the intact bone specimens . . . . . 86

# NOMENCLATURE

$a_n$ $\Re$ *Fourier coefficient*

$b_n$ *imaginary Fourier coefficient*

$c$ *damping constant*

$c_c$ *critical damping*

$E$ *modulus of elasticity*

$e$ $\ln e = 1$ $(e \approx 2.71828)$

$G$ *power spectrum*

$g$ *acceleration of gravity*

$H_{(\omega)}$ *transfer function*

$I$ *area moment of inertia*

$k$ *stiffness spring constant*

$M$ *moment*

$m$ *mass*

$P$ *force*

$t$ *time*

$v$ *deflection*

$\epsilon$ *strain*

$\kappa$ *curvature*

$\rho$ *radius of curvature*

$\sigma$ *stress*

$\omega_n$ *natural frequency*

$\zeta$ *damping ratio*

# CHAPTER I

# INTRODUCTION

## Problem Statement

Fractures are a significant medical problem. There are a wide variety of treatment options to assist the bone in its healing. These options have focused on improvement of the mechanical environment and range from simple external supports to sophisticated and expensive surgical devices. Bone as a living tissue has a remarkable capacity to regenerate itself. However, this process can take considerable time. During this healing period the involved limb is nonfunctional which contributes to the morbidity associated with fractures. This morbidity includes joint stiffness, atrophy of muscles and loss of strength. The longer the inactivity, the worse the complications. This is especially true when the healing of bone is delayed or ceases. In such cases the risk for serious and permanent disability is increased.

Much effort has been placed in developing operative methods and materials to enhance the healing so that the mechanical function of the bone can be quickly restored. More recently attention has been focused on the cellular and biochemical levels. For example, growth hormone (somatotropin) has been found to have a profound effect on the quality of bone healing.

Even though the bone's major function is mechanical, there are no practical, noninvasive means of assessing, in vivo, the mechanical properties of bone. At the present

time, healing bones are assessed qualitatively by interpreting radiographic and clinical signs. Assessments made by these methods may not always be accurate with respect to the actual mechanical behavior of bone. A noninvasive in vivo mechanical test would compliment present qualitative clinical assessments.

## Research Applications

Although fracture research is focusing on the enhancement of callus formation by biologic means, still a reliable in vivo method for the quantitative assessment of fracture callus stiffness and strength is needed. Vibrational analysis may be well suited for such a challenge.

Of the various biological factors studied, exogenous growth hormone, somatotropin, has a strong influence on the quality and rate of healing (Millis et al, 1998). Radiographic interpretation, bone mineral density scans, weight bearing analysis, histochemistry, and destructive testing all were used to evaluate somatotropin's influence. However, load deformation curves are more definitive for evaluating mechanical characteristics such as strength and stiffness of a healing bone, but they require death of the subject and removal of the bone for testing. In the live subject there are no well established methods that can evaluate such characteristics. A noninvasive method that would yield quantifiable data on the strength and stiffness of healing bone would make it possible to evaluate the process throughout the healing period without destroying the animal subject.

## Clinical Applications

Many fracture treatment methods have been developed over the past 50 years. They include the use of metallic implants, resorbable implants, external implants, electrical stimulation, and coaptation supports. All of these have the potential to influence the quality of healing. Managing the fracture patient is an inexact science. Clinical judgements are based on experience, radiographic interpretation and the presentation of clinical signs or symptoms. Clinical problems such as stress protection, disuse osteoporosis, premature implant removal, immobilization or controlled motion cannot be fully addressed without understanding the mechanical status of the healing bone. A noninvasive method of assessing fracture callus strength in the live patient would assist the orthopedist in the decision making process.

## Hypotheses

Vibrational analysis can yield two parameters, natural frequency and damping, that can be useful in assessing the mechanical characteristics of bone. The natural frequency of a system is related to the stiffness and mass of the system. A fracture callus forms in 6 - 8 weeks and provides an interim measure of stability for the bone to fully reconstitute itself which may take as long as a year. Since a healing bone is not as rigid or stiff as an intact bone, it is proposed that the natural frequency of an intact bone is significantly larger than that of a healing calloused bone.

During the progressive stages of healing, the callus will steadily increase in stiffness especially under the influence of somatotropin. It is proposed that the natural frequencies will be significantly different between bones with a poor healing callus and those stimulated by growth hormone. It is further proposed that the difference in the natural frequencies will positively correlate with the differences demonstrated by the standard load deformation curves.

A system placed in free vibration will eventually stop oscillating due to energy dissipation. This loss of energy is termed damping. Unstable ostectomized bones will quickly dissipate energy when compared to stable intact bones. It is proposed that intact bones will be lightly damped while the ostectomized bones will be more heavily damped. A callus without somatotropin influence should be less rigid and show more damping than those exposed to somatotropin. Therefore, it is proposed that damping will be different among the somatotropin treatment groups. Also it is proposed that damping will positively correlate with the changes demonstrated by the standard load deformation curves.

# CHAPTER II

# REVIEW OF THE LITERATURE

## Growth Hormone and Fracture Healing

Bone has a tremendous capacity to heal and reconstitute itself. As a biological tissue it is unique in its ability to grow like soft tissue but unlike soft tissue it can harden to a point where it can bear substantial mechanical loads. Fracture healing has long been a focus of study as many methods of treatment have been advanced. These efforts have typically focused on improving the mechanical environment of the fracture. Recently the interest has expanded to the cellular and biochemical level. While it is understood that the cell is the basic engine of repair, the cell is modulated by its environment and by chemical mediators. This new attention has been focused on biochemical substances or growth factors that are capable of modulating cell function. These growth factors are in turn controlled by hormones. In the case of bone healing, growth hormone (somatotropin) has a profound effect (Bak, 1993; Millis et al, 1998).

A number of tissue growth factors have been identified. Bone morphogenic protein (Urist et al, 1983) and human skeletal growth factor (Farley and Baylink, 1982) have been isolated and studied. Bone morphogenic protein stimulates precursor cells to differentiate into bone producing cells. Human skeletal growth factor stimulates the differentiated cells

to produce bone. Somatotropin can exert its effect directly on bone cells and indirectly through insulin-like growth factor (Denis, 1994).

The formation of a bridge to unite and stabilize the ends of a fractured bone involves a variety of compounds, tissues and sophisticated mechanisms. The resulting composite is the fracture callus. After the callus has formed, the physiology shifts to a remodeling mode. In this mode the bone reconstitutes itself but is still under the influence of these growth factors and their effects on target cells.

Growth hormone or somatotrophin is secreted from the anterior pituitary gland in the brain. Somatotropin has multiple sites of effects, but this investigation will concentrate on those specific effects on bone. Early studies discovered that extracts of the pituitary gland did have a stimulatory effect on the production of bony callus (Bak, 1993). However, not all subsequent studies showed a positive effect. Many of the negative results were attributed to problems associated with growth hormone preparation, delivery and dosage. Also the lack of species specific growth hormone contributed to poor results. Because of recent developments of genetic engineering and recombinant technology, species specific growth hormone is now available.

The influence of growth hormone has been observed clinically as well as experimentally. For example, low growth hormone levels have been reported in patients with delayed union fractures (Misol et al, 1971). In some clinical cases, parenteral administration of human growth hormone resulted in the healing of nonunion fractures (Ahl and Kalen, 1979). However, the use of somatotropin is still primarily experimental.

Research experience in the effect of somatotropin has been varied. For example, no effect was seen following removal of the anterior pituitary in rat (Wray and Goldstein, 1966). Also, in this study, the replacement of growth hormone did not help. On the other hand, mice with hereditary deficient anterior pituitaries had considerable difficulty in healing fractures (Hsu and Robinson, 1969). Other studies in mice (Shepanek, 1953), in rabbits and rats (Herold et al, 1971) did not show a beneficial effect. Successful studies were reported in rats (Udupa and Gupta, 1965; Tylkowski et al, 1976; Nothmore-Ball et al, 1980) and in mice (Ashton and Dekel, 1983). Mature dogs with bone gaps that would not heal normally healed under the influence of growth hormone (Zadek and Robinson, 1961). In addition to fracture studies, cortical bone elasticity has also been studied. It was found that under the influence of human recombinant growth hormone the elastic modulus of aged bone was increased (Kohles et al, 1996).

In a more recent study, *E coli* derived human growth hormone was administered to rats with experimentally induced tibial fractures (Bad, 1993). In this study it was found that fracture healing was significantly increased in the early part of the fracture healing period, specifically the first 40 days. This supports the theory that growth hormone targets the cartilage cell which functions primarily in early callus formation. In addition to this finding, it was determined that growth hormone was beneficial to the old rat in which bone healing is normally reduced. In the case of the old rat the hormone was given early in the healing period but the effect was not realized until 80 days into the healing process. This study utilized three point bending tests in determining the beneficial effect of somatotropin.

In two recent comprehensive studies involving dogs, the administration of recombinant canine growth hormone demonstrated a beneficial effect in the stimulation of bone healing (Wilkens et al, 1996; Millis et al, 1998). Partial radial ostectomies were done to produce delayed or nonunion fractures. As determined by histologic evaluation, the healing of ostectomies exposed to canine somatotropin was far more advanced than those not exposed. Biomechanical tests and bone mineral content studies further documented the value of recombinant canine growth hormone administration. It is also important to note that in these studies the hormone was administered in a continuous fashion through an osmotic pump surgically placed in the subcutaneous muscular tissues.

## Evaluation of Fracture Healing

The evaluation of bone for strength and stiffness can be patterned after that for beams. Analysis for bone must consider that bone is anisotropic and nonhomogeneous. These characteristics are manifested more in the case when the bone is healing with a callus. The composite of tissue types in the callus makes the bone more nonlinear and less predictive in its mechanical behavior. The callus also changes over time. The concentration of calcium per unit volume of callus which represents the mineral content increases four times over the course of callus development. The hydroxyproline concentration which represents the proteinaceous fiber content doubles within the callus as the bone heals. Finally the breaking strength of the callus at its most mature stage is three times that of the initial callus (Chao and Aro, 1991). Some have stated that the most reliable method of fracture strength

determination is the tensile test (Chao and Aro, 1991), but it is obviously not suitable for in vivo evaluation.

There are four stages of fracture callus development that can be mechanically defined (Chao and Aro, 1991). In Stage I, the fracture callus fails at its original site in a highly elastic rubbery pattern with low stiffness. Stage II is characterized by failure through the callus but there is increased stiffness and the load pattern is similar to hard tissue. In Stage III, the bone fails partly through the callus at the original site of fracture and partly through the adjacent bone. In Stage IV, the fully developed callus exhibits great strength as the bone fails through the adjacent bone and not through the callus.

Three point bending tests have been done for healing bone under the influence of growth hormone (Bad, 1993; Millis et al, 1998). Some problems do complicate deformation testing; for example, standardized specimens of a fracture callus cannot be obtained due to the composite of tissue types that are randomly scattered throughout the callus. Also the irregular geometry of the callus makes the mathematical prediction of stress and strain difficult. Uneven distribution of stress and strain further complicates the testing process. Some have investigated bending, tensional, and torsional testing in rat bones and found that bending was the most practical. Three point bending was selected in some studies so that the force could be applied directly at the weakest point which is the callus. While this concentrates the failure at the callus it does introduce shear forces across the bone. Not only does the location but also the direction of the applied load affect the response in the bone. Differences in strain rates also affect the mechanical behavior of bone in that higher strain rates will increase stiffness and maximal failure values.

An additional concern for testing bone is in the preparation of the bone itself. It is well known that wet and dry bones perform differently. In the previous studies cited, bone specimens were stored in balanced electrolyte solutions and refrigerated (Bad, 1993).

## Vibrational Analysis of Fracture Healing

There are noninvasive methods for evaluating bone. These techniques have been classified into two groups; radiation absorption methods and vibratory methods (Katz and Yoon, 1975). The radiation absorption group includes X-ray photodensitometry, quantitative computed tomography, single photon absorptiometry and dual energy X-ray absorptiometry. In the vibratory group there is resonance frequency and impedance, ultrasound propagation, and computed tomography of ultrasound energy. Absorptiometry techniques can assess bone healing by evaluating the concentration of minerals in the fracture callus (Markel and Bogdanske, 1994). Vibratory methods assess bone healing by evaluating sound transmission (Ricciardi et al, 1993; Fellinger et al, 1994) or inducing vibration and recording an acceleration response. At the present time, Markel states that of all these techniques, computed tomography of ultrasound energy, quantitative computed tomography, single photon absorptiometry, and dual energy X-ray absorptiometry have the greatest potential for noninvasive fracture strength evaluation (Markel and Chao, 1993).

Most vibratory tests involve the application of force to the test specimen and recording a response. There are principally two ways of testing in this manner, first an impact hammer test which delivers a unit force, and second a sinusoidal excitation test which

delivers a continuous harmonic force. Beam analysis forms a basis for the evaluation of long bones by vibrational methods. The theoretical relationship between resonant frequencies and torsional stiffness was explored in the development of a formula that with the mass and length of the bone known, the torsional stiffness can be derived from the natural frequencies (Lowet et al, 1993). However, there are several problems associated with these types of tests. For example, when bones are tested in situ, the presence of soft tissue around the bone attenuates the response. Also the presence of soft tissue makes the consistent and stable placement of transducers and shakers more difficult (Orne, 1974). These problems along with the irregular geometry of the bone create difficulties in obtaining consistent data and in the accurate extraction of mechanical parameters.

Several investigations have been carried out on specific long bones to determine the feasibility of extracting meaningful mechanical parameters from vibrational testing (Van-der-Pere et al, 1983; Christensen et al, 1986; Cornelissen et al, 1986 and 1987; Steele et al, 1988; Thomsen, 1990). Human ulnar stiffness was determined in vivo by a vibratory method called "Mechanical Response Tissue Analysis". In this analysis, resonant frequencies were not used as the comparative parameter but the impedance curve which is a description of force to velocity was converted to a curve of force to displacement from which the stiffness parameter was extracted. Favorable comparisons were obtained between the stiffness of the ulna obtained from this in vivo test and in the vitro tests done by three point bending (Steele et al, 1988). In the study of excised human tibias and corresponding mathematical models, seven natural frequencies of the human tibia have been described. The mathematical models

suggested that the tibia is more uniform in its vibrational response than expected when considering the varied geometry of the bone (Thomsen, 1990).

Several considerations are necessary when testing bones in situ. Some investigations concluded that the excitation techniques and the methods of signal processing had little effect on the consistent determination of natural frequencies and mode shapes, whereas the supporting conditions had a larger effect on these parameters (Christensen et al, 1986). Also involved with in situ testing is the influence of the soft tissue envelope. The surrounding soft tissue, especially the muscle, has a profound effect on the determination of natural frequencies by adding significant mass and damping to the system (Van-der-Pere et al, 1983; Cornelissen et al, 1986). Even the soft tissue within the bone contributes significantly to the vibratory response in that the differences observed between the response of dry vs wet bone has been attributed to the absence of the marrow tissues in the dry bone (Van-der-Pere et al, 1983). Interestingly, the joints and skin played a lesser role in these studies.

Through vibratory modal analysis, some bending modes have been described for the human tibia which occur at approximately 350 Hz and 550 Hz (Cornelissen et al, 1987). Also, in excised human tibias, seven natural frequencies have been determined (Thomsen, 1990). Based on these analyses finite element models of the human tibia have been developed. A three dimensional finite element model of the human tibia was developed that could predict modal parameters with a 3% relative error when compared to experimentally derived parameters (Hobatho et al, 1991). Other projects have used finite element models to predict the effect of variable mass and geometry, rotary inertia and shear deformation on modal parameters (Orne, 1974).

These parameters such as natural frequencies and mode shapes do contribute to the understanding of how the bone responds to mechanical loading (Thomsen, 1990). This fact becomes useful in the monitoring the rate and quality of the healing of fractured bones. Through experimental vibrational tests and the use of credible finite element models, considerable variation in the upper natural frequencies do occur as healing progresses (Laura et al, 1990). Other studies have investigated the change in the vibratory character of the bone finding that vibration indeed described the asymmetric weakening of the bone as it was progressively transected (Cornelissen et al, 1987). Still others have demonstrated the usefulness of using resonant frequencies in assessing fracture healing, noting that in general these frequencies increase as the fracture heals and becomes more rigid (Van-der-Pere et al, 1983; Richards, 1987; Cornelissen et al, 1987; Benirschke et al, 1993; Lowet et al, 1996). In addition to increasing bending stiffness, natural frequencies were also found to increase in a linear fashion with increasing torsional stiffness in healing bone (Lowet et al, 1996). Along with natural or resonant frequencies, mode shapes have also been studied. For example, single bending modes were more prominent in bones with the callus in the center of the diaphysis while double bending modes were more sensitive in bones where the callus was in a distal location (Lowet et al, 1996).

Limited clinical application has been made. From vibrational analysis of an excised human tibia, the natural frequency and mode shapes were determined in two planes, ie laterally and axially. In the intact tibia, response data was not coupled between the lateral and axial tests. To simulate a healing bone, an excised tibia was excised and weakly repaired with an epoxy resin. This artificial union was progressively strengthened and then tested

vibrationally. Initially, when the union was weak, the natural frequency was low; but as the union increased in stiffness, the natural frequency increased. When a clinical fracture case was subsequently tested, the presence of the soft tissue envelope and an external cast made the definition of the separate natural frequencies difficult. In spite of this difficulty and unlike the intact bone, there was a coupling of the response data between the lateral and axial responses confirming the presence of nonuniform healing and a delayed union fracture (Nikiforidis et al, 1990).

Vibrational analysis can provide a noninvasive study of the mechanical characteristics of the long bones. This type of analysis parallels mechanical analysis as the relationship between the stiffness and natural frequency is established by experimental and mathematical modelling. Although there are still problems associated with the obtaining and interpreting vibration data, it is with this background that the development of noninvasive mechanical analysis by the vibratory method continues.

# CHAPTER III

# THEORETICAL BASIS

## Beam Analysis

A beam is defined as a structure with forces acting transversely to its longitudinal axis. A cantilever beam is a special case where it is fixed at one end where force and moment reactions can occur and free at the opposite end where it can physically translate and rotate. Although loads on the beam can be concentrated or distributed, this analysis will consider a concentrated load on the free end of a cantilever beam. The purpose for this discussion is the development of an expression for the deflection a cantilever beam with a concentrated load on its free end.

### *Curvature and Deflection*

Curvature is mathematically described as the inverse of the radius of curvature and is called "kappa":

$$\kappa = \frac{1}{\rho}$$

Curvature is related to the incremental change in the angle of curvature and the deflection of the beam at its free end by:

$$\kappa = \frac{d\theta}{dx} = \frac{d^2v}{dx^2}$$

***Curvature and Flexural Rigidity***

The normal strains in the deflecting beam are related to the curvature by:

$$\epsilon_x = -\kappa y$$

Assuming that the beam is linearly elastic, the normal stresses can be derived from the normal strains by Hooke's Law which states that stress is related to strain via the proportionality constant "E" which is Young's modulus. For this case the following relationship between stress and strain is:

$$\sigma_x = E\epsilon_x = -E\kappa y$$

The end load at the free end of the beam that created a bending moment at the fixed end is the source of the normal stress within the beam:

$$-\sigma_x = \frac{dM}{ydA}$$

The resultant moment in the beam is:

$$M = -\int \sigma_x y dA$$

Utilizing Hooke's Law the resultant moment can be expressed as:

$$M = -\kappa E \int y^2 dA$$

The integral in the above formula is actually the moment of inertia of the cross section which is defined as:

$$I = \int y^2 dA$$

Using "I" for the moment of inertia, the equation can be rewritten as:

$$M = -\kappa EI$$

and solving for curvature to obtain:

$$\kappa = \frac{1}{\rho} = -\frac{M}{EI}$$

The quantity "EI" is unique to the composition and geometry of the beam and is commonly referred to as the flexural rigidity of the beam.

*Deflection of Cantilever Beam*

From the proceeding equations, one sees that the curvature of the cantilever beam is related to deflection by:

$$\kappa = \frac{d^2v}{dx^2}$$

and to flexural rigidity by:

$$\kappa = -\frac{M}{EI}$$

Therefore, these two relationships can be combined into a second order differential equation describing the deflection of a beam:

$$\frac{d^2v}{dx^2} = -\frac{M}{EI}$$

Solving this differential equation for the deflection of an end loaded cantilever beam:

$$v = \frac{Px^2}{6EI}(3a-x)$$

At the free end of the beam the deflection reduces to:

$$v = \frac{PL^3}{3EI}$$

# Vibrational Analysis

## *Natural Frequency and Flexural Rigidity*

Vibration can be free or forced. Under free vibration a system will vibrate at one or more of its natural frequencies. Natural frequencies are determined by the mass and stiffness characteristics of the system. Under forced vibration, if the frequency of the excitatory force equals that of the natural frequency, the amplitude of the vibration will increase until the system fails. This constitutes the state of resonance.

The dissipation of energy in a vibrating system is referred to as damping. Damping is also related to mass and stiffness.

The purpose of this discussion is to develop the relationship between the natural frequency of a beam and its flexural rigidity, define damping, the frequency response function and to describe the application of Fourier analysis.

Harmonic motion can be pictured as a point moving on a circle. The track of this moving point can be projected onto an x and y coordinate graph. On the coordinate axis, the track of this moving point will appear as a repeating sine or cosine function. Since this motion is repetitive, there is a period of time at which the motion is repeated. Based on this description the position of the moving point, "x" is determined by:

$$x = A\sin 2\pi\frac{t}{\tau}$$

where

$$\tau = period\ of\ repitition$$

$$A = Amplitude$$

An additional consideration is the speed which the point has on the circle. This speed can be considered as a circular frequency and is expressed as:

$$\omega = \frac{2\pi}{\tau}$$

Substituting circular frequency into the basic description of harmonic motion yields:

$$x = A\sin\omega t$$

This equation for motion can be appropriately differentiated to yield expressions for velocity:

$$\frac{dx}{dt} = \omega A\cos\omega t$$

and for acceleration:

$$\frac{d^2x}{dt^2} = -\omega^2 A\sin\omega t$$

The expression for acceleration can be rewritten by using the above expression for x, therefore:

$$\frac{d^2x}{dt^2} = -\omega^2 x$$

The above expression clearly relates acceleration to the displacement.

Harmonic motion can be modeled as a mass suspended on a spring with a spring constant "k". The force in the spring is proportional to displacement:

$$F = k(\Delta x)$$

At static equilibrium the weight of the mass is equal to the spring force:

$$mg = k(\Delta x)$$

Newton's second law of motion dictates that acceleration is proportional to force. Applying both Newton's second law of motion and the condition of static equilibrium the equation of motion is:

$$\Sigma F = mg - k(\Delta x - x) = m\frac{d^2x}{dt^2}$$

Noting that at equilibrium the spring force is equal to the weight of the mass the equation of motion becomes:

$$\frac{d^2x}{dt^2} = -\frac{k}{m}x$$

Therefore:

$$\omega^2 = \frac{k}{m}$$

Thus the equation of harmonic motion in terms of circular frequency is:

$$\frac{d^2x}{dt^2} + \omega^2 x = 0$$

Solving this second degree homogenous differential equation for x:

$$x = A\sin\omega_n t + B\cos\omega_n t$$
$$\omega_n = Natural\ Frequency$$

The natural frequency is the frequency that the system will naturally assume in the state of free vibration. This frequency is unique to the system and is related to the spring constant "k" and the mass "m" of the system. Considering that a beam can act as a spring, the deflection of the beam can be described in terms of a spring constant. The expression for the deflection of a cantilever beam with an end load "P" is:

$$v = \frac{PL^3}{3EI}$$

Solving for the force P:

$$P = \frac{3EI}{L^3} v$$

Note that the force "P" is related to the deflection just as a spring force is related to the

deflection of the spring via a proportionality constant which in the case of a cantilever beam with a concentrated end load is:

$$k = \frac{3EI}{L^3}$$

Therefore, for the harmonic vibration of a cantilever beam with a concentrated load on the free end, the natural frequency is:

$$\omega_n = \sqrt{\frac{3EI}{L^3 m}}$$

Therefore by the above relation, the natural frequency of a harmonically vibrating beam is related to the flexural rigidity of the beam.

***Damping***

Damping is the dissipation of energy during oscillation. In the mass and spring model of free harmonic vibration, a dashpot can be added to model the effects of damping. The force exerted by the dashpot is proportional to the velocity via a damping constant "c":

$$F_d = c\frac{dx}{dt}$$

The equation of motion for this mass, spring and dashpot model of free vibration is:

$$m\frac{d^2x}{dt^2} + c\frac{dx}{dt} + kx = 0$$

For this homogeneous second order differential equation the solution form is:

$$x = e^{st}$$

Substituting the solution form into the differential equation yields:

$$(ms^2+cs+k)e^{st} = 0$$

All values of t are satisfied when:

$$s^2+\frac{c}{m}s+\frac{k}{m} = 0$$

Solving this quadratic equation for s, there are two roots:

$$s_{1,2} = -\frac{c}{2m}\pm\sqrt{(\frac{c}{2m})^2-\frac{k}{m}}$$

Substituting the expressions for s into the general solution:

$$x = Ae^{s_1t}+Be^{s_2t}$$

$$x = e^{-(\frac{c}{2m})t}\,[Ae^{\sqrt{(\frac{c}{2m})^2-\frac{k}{m}}\,t} + Be^{-\sqrt{(\frac{c}{2m})^2-\frac{k}{m}}\,t}]$$

The first term in the general solution is a decaying exponential. The influence of the second term (brackets) depends upon the sign of the quantity within the radical. The quantity

containing the damping constant is referred to as the damping term:

$$(\frac{c}{2m})^2$$

If the damping term is greater than (k/m) then the quantity within the radical is positive and the numbers are real. Under this condition there are no oscillations and the system is classified as overdamped. If the damping term is less than (k/m) then the quantity is negative and the exponent becomes imaginary. Under these conditions oscillations occur and the system is considered to be underdamped. The limiting case between oscillatory and non-oscillatory motion occurs when the damping factor equals (k/m). This limiting case is referred to as critically damped.

Damping is typically expressed as a ratio where the damping constant is divided by the critical damping constant:

$$\zeta = \frac{c}{c_c}$$

***Frequency Response Function***

Thus far, unforced free harmonic vibration has been considered. The analysis now can be expanded to include the spring, mass, damper model with an external force that stimulates the vibration. The equation of motion is similar except that it becomes a

nonhomogeneous second order differential equation with a forcing function:

$$m\frac{d^2x}{dt^2}+c\frac{dx}{dt}+kx = F_0\sin\omega t$$

The particular solution assumes the following form:

$$x = X\sin(\omega t-\phi)$$
$$X = Amplitude$$
$$\phi = phase\angle$$

Substituting into the differential equation and solving for amplitude:

$$X = \frac{F_0}{\sqrt{(k-m\omega^2)^2+(c\omega)^2}}$$

In the dimensionless form (dividing by k):

$$X = \frac{\frac{F_0}{k}}{\sqrt{(1-\frac{m\omega^2}{k})^2+(\frac{c\omega}{k})^2}}$$

Solving for the phase angle:

$$\tan\phi = \frac{\frac{c\omega}{k}}{1-\frac{m\omega^2}{k}}$$

Defining:

Natural frequency of undamped vibration:

$$\omega_n = \sqrt{\frac{k}{m}}$$

Critical damping:

$$c_c = 2m\omega_n$$

Damping ratio:

$$\zeta = \frac{c}{c_c}$$

and:

$$\frac{c\omega}{k} = \frac{c}{c_c}\frac{c_c\omega}{k} = 2\zeta\frac{\omega}{\omega_n}$$

Substituting the above definitions into the expression for the amplitude:

$$\frac{Xk}{F_0} = \frac{1}{\sqrt{[1-(\frac{\omega}{\omega_n})^2]^2+[2\zeta(\frac{\omega}{\omega_n})]^2}}$$

A curve with peak values occurring at resonant frequencies is produced when the amplitude is plotted against the frequency ratio. The frequency at the resonant peak is equal to the natural frequency.

Solving for the phase angle:

$$\tan\phi = \frac{2\zeta(\frac{\omega}{\omega_n})}{1-(\frac{\omega}{\omega_n})^2}$$

When the phase angle is plotted against the frequency ratio, a major shift in the phase angle occurs at the resonant point.

The complete solution:

$$x_{(t)} = \frac{F_0}{k}\frac{\sin(\omega t-\phi)}{\sqrt{[1-(\frac{\omega}{\omega_n})^2]^2+[2\zeta\frac{\omega}{\omega_n}]^2}} + X_1 e^{-\zeta\omega_n t}\sin(\sqrt{1-\zeta^2}\omega_n t+\phi_1)$$

The above expressions can be rewritten in the complex form utilizing Euler's equation:

$$e^{i\theta} = \cos\theta + i\sin\theta$$

A sinusoidal forcing function can then be written as a complex sinusoid:

$$F_0(\cos\omega t + i\sin\omega t) = F_0 e^{i\omega t}$$

The amplitude can be written as a complex displacement vector:

$$\overline{X} = Xe^{-i\phi}$$

and the displacement as:

$$x = Xe^{i(\omega t-\phi)} = (Xe^{-i\phi})e^{i\omega t} = \overline{X}e^{i\omega t}$$

Substituting into the differential equation of motion and simplifying:

$$(-\omega^2 m + ic\omega + k)\overline{X} = F_0$$

The solution can be written as:

$$\overline{X} = \frac{F_0}{(k-\omega^2 m)+i(c\omega)} = \frac{\frac{F_0}{k}}{1-(\frac{\omega}{\omega_n})^2+i(2\zeta\frac{\omega}{\omega_n})}$$

Forced vibration is commonly assessed by dividing the output by the input information. This relationship between input and output is called the Complex Frequency Response Function (Transfer Function):

$$H(\omega) = \frac{\overline{X}}{F_0} = \frac{\frac{1}{k}}{1-(\frac{\omega}{\omega_n})^2+i2\zeta\frac{\omega}{\omega_n}}$$

The real and imaginary components of the Complex Frequency Response Function can be separated apart by multiplying and dividing the above equation by the complex

conjugate of the denominator obtaining:

$$H(\omega) = \frac{1-(\frac{\omega}{\omega_n})^2}{[1-(\frac{\omega}{\omega_n})^2]^2+[2\zeta\frac{\omega}{\omega_n}]^2} - i\frac{2\zeta\frac{\omega}{\omega_n}}{[1-\frac{\omega}{\omega_n})^2]^2+[2\zeta\frac{\omega}{\omega_n}]^2}$$

At resonance:

$$\omega = \omega_n$$

At resonance, the real part of the complex frequency response is zero and the response is attributable to only the imaginary part. Therefore, at resonance where the Complex Frequency Response Function reduces to:

$$H(\omega) = -i\frac{1}{2\zeta}$$

At resonance the phase angle is 90 degrees noting that the tangent function is undefined at resonance:

$$\tan\phi = \frac{2\zeta\frac{\omega}{\omega_n}}{1-(\frac{\omega}{\omega_n})^2}$$

### *Fourier Analysis*

The theoretical basis for the analysis of harmonic motion has been described in terms of natural frequency, damping, and frequency response function. However, naturally occurring vibration is not generally harmonic but random. There are techniques to capture these complex wave forms and analyze them for the purpose of extracting parameters of importance such as natural frequency and damping.

Any periodic function can be represented by the sum of a series of cosine and sine functions. Such a series is called the Fourier series:

$$x_{(t)} = a_0 + \sum_{n=1}^{\infty} (a_n \cos n\omega_0 t + b_n \sin n\omega_0 t)$$

where

$$\omega_0 = 2\pi f = \frac{2\pi}{\tau}$$
$$\tau = period$$
$$\omega_0 = fundamental\ frequency$$

The coefficients of each of the trigonometric functions determine the behavior of the individual wave forms represented by the series. It becomes important to determine the value of these coefficients. Considering the fact that these terms of the series are orthogonal, the constants can be evaluated by:

$$a_n = \frac{2}{\tau} \int_{-\frac{\tau}{2}}^{\frac{\tau}{2}} x_{(t)} \cos\omega_n t dt$$

$$b_n = \frac{2}{\tau} \int_{-\frac{\tau}{2}}^{\frac{\tau}{2}} x_{(t)} \sin\omega_n t dt$$

It is convenient to convert the terms of the Fourier series into the complex form utilizing Euler's formula:

$$\cos\omega_n t = \frac{1}{2}(e^{i\omega_n t} + e^{-i\omega_n t})$$
$$\sin\omega_n t = -\frac{1}{2}(e^{i\omega_n t} + e^{-i\omega_n t})$$

where:

$$\omega_n = n\omega_0 = \frac{n2\pi}{\tau}$$
$$\omega_0 = \textit{fundamental frequency}$$
$$\omega_n = \textit{harmonic (multiple of fundamental frequency)}$$

Substituting these rewritten terms into the Fourier series:

$$x_{(t)} = \frac{a_0}{2} + \sum_{n=1}^{\infty}[\frac{1}{2}(a_n - ib_n)e^{i\omega_n t} + \frac{1}{2}(a_n + ib_n)e^{-i\omega_n t}]$$

Collecting terms:

$$x_{(t)} = \sum_{n=-\infty}^{\infty} c_n e^{-i\omega_n t}$$

Now substituting in the solutions for the "a" and "b" coefficients and solving for "c":

$$c_n = \frac{1}{\tau}\int_{-\frac{\tau}{2}}^{\frac{\tau}{2}} x_{(t)} e^{-i\omega_n t} dt$$

The Fourier series contains both the real and imaginary parts which are used to assemble a frequency response function. Those coefficients are:

$$a_n = realpart$$
$$b_n = imaginary\ part$$

Note also that these coefficients are orthogonal to each other thus:

$$|2c_n| = \sqrt{a_n^2 + b_n^2}$$

The phase angle can also be determined from these coefficients:

$$phase\angle = \tan^{-1}\frac{b_n}{a_n}$$

While the Fourier series was developed to represent periodic wave motion, it can also be used to describe random wave motion by changing the period from finite time to infinity. By applying the above complex integral to an infinite period of time a function (Fourier Integral) in the frequency domain is produced describing this random wave:

$$X_{(\omega)} = \int_{-\infty}^{\infty} x_{(t)} e^{-i\omega_n t} dt$$

While the Fourier Integral can take the function in the time domain and convert it to a function in the frequency domain, the inverse of the Fourier Integral can convert the

frequency dependent function back to the time dependent function:

$$x_{(t)} = \int_{-\infty}^{\infty} X_{(\omega)} e^{i\omega_n t} d\omega$$

The above pair of integrals are sometimes referred to the as the Fourier Transform. These two integrals form the basis for the ability of the analyzer to obtain time domain data of a random wave form and convert it into a frequency based function.

In spite of the random nature of vibration, random wave forms do exhibit some statistical regularity. There are some mathematical techniques that can capture this regularity such that analysis and parameter estimation can be made. The mean of a random function can be defined as:

$$\overline{x_{(t)}} = \lim_{T\to\infty} \frac{1}{T} \int_0^T x_{(t)} dt$$

The mean square value is:

$$\overline{x_{(t)}^2} = \lim_{T\to\infty} \frac{1}{T} \int_0^T x_{(t)}^2 dt$$

The fluctuation of the mean square value about the mean is the variance and is defined as:

$$\sigma^2 = \lim_{T\to\infty} \frac{1}{T} \int_0^T (x_{(t)} - \overline{x_{(t)}})^2 dt$$

A sample is a time record of the random function. If these statistical values are constant regardless of the start time for the sample, the random function is considered stationary. If these statistical values are constant for all samples in an ensemble then the random function is ergodic. The signal analyzer utilizes random functions that fulfill these statistical characteristics.

The value of the Fourier coefficients used by the analyzer is the mean square value of the individual harmonic. The mean square value is made up of individual contributions in each frequency interval. These contributions are the coefficients multiplied by their complex conjugates. This square value is the power spectrum. An input and a separate output spectrums can be calculated. Power spectral data exclude the phase information. Cross spectrums produced by multiplying the input spectrum by the conjugate of the output spectrum do retain phase information. The analyzer utilizes these power spectrums to create the frequency response function:

$$H_f = \frac{G_{XY}}{G_{XX}}$$

where

$$H_f = \textit{Transfer Function}$$
$$G_{XY} = \textit{Cross Spectrum}$$
$$G_{XX} = \textit{Input Power Spectrum}$$

Since it is not possible for the analyzer to use infinity as the sample period, the Discrete Fourier Transform is used and is the application of the Fourier Transform over a discrete window of time:

$$X_{(k\Delta f)} = \Delta t \sum_{n=0}^{N-1} x_{(n\Delta t)} e^{-i2\pi k\Delta f n\Delta t}$$

where:

$$N = \textit{number of samples}$$
$$\Delta t = \textit{sampling interval}$$
$$\Delta f = \frac{1}{N\Delta t} \textit{ sample interval; frequency domain}$$
$$n = \textit{time sample index}$$
$$k = \textit{frequency sample index}$$
$$x_{(n\Delta t)} = \textit{set of time samples}$$
$$X_{(k\Delta f)} = \textit{set of Fourier coefficients}$$

While the discrete Fourier Transform allows for the computation of Fourier coefficients of random oscillatory motion, the number of calculations required makes it impractical except by way of computer algorithm. The Fast Fourier Transform is the algorithm that makes the application of the Discrete Fourier Transform a practical procedure.

## Summary

The equations of motion of an end loaded cantilever beam are related to the equations of motion of a vibrating cantilever beam by means of stiffness and mass. Periodic motion can be described by means of a trigonometric series called the Fourier series. Random vibration can be evaluated by considering random wave motion to be periodic with infinity. This led to the development of the Fourier Integral. A pair of Fourier integrals (one being the inverse of the other) constitute the Fourier Transform. By the use of the Fourier transform, random wave forms observed in time can be described in the frequency domain. The Fourier Transform can be applied to discrete time samples by the Discrete Fourier Transform which is efficiently calculated by the Fast Fourier Transform algorithm.

# CHAPTER IV

# MATERIALS AND METHODS

## Design

The vibrational testing protocol was part of an overall investigation designed to determine the ideal time of treatment of somatotropin treatment for fracture healing in the dog.

Sixteen healthy adult Beagle dogs were divided into four treatment groups. These treatment groups were selected on the basis of duration of exposure to canine somatotropin. One group was exposed for 3 weeks, one for 6 weeks, one for 12 weeks and a control group had no exposure.

By random selection, the right or left radius was partially ostectomized in each dog. Under general anesthesia the ostectomy was performed through a 3 cm incision directly over the midshaft of the radius. A small section of the radius approximately 3 mm in length was removed from the shaft. The tissues were closed in a routine fashion. The ulna was left intact which provided some stability and function to the leg. Provision for pain relief was made through the administration of analgesics.

Recombinant canine somatotropin hormone was supplied in an implantable cylinder which by an osmotic process delivered the hormone on a continuous basis. The osmotic pump was implanted into the subcutaneous tissue space in the back between the scapulae.

Preoperatively each dog was examined and radiographed to assure that the animal was in good health and the bone was normal. Also each dog was screened with dual energy x-ray absorptiometry (DEXA) to evaluate bone mineral density.

Postoperatively each dog was followed with radiographs and DEXA scanning to evaluate the quality of fracture healing. At the end of the study each dog was humanely euthanatized. Each healing radius and its contralateral intact radius was harvested for mechanical testing and histologic evaluation. Vibrational testing was done just prior to the three point bending tests. The objective of vibrational testing was to investigate the potential for this mode of testing in discriminating between poor and good healing fractures.

After the harvesting, each radius was wrapped in a saline soaked gauze sponge and stored on ice until tested. Mechanical testing took place within 24 hours of harvesting. Prior to testing, each sample was potted in dental acrylic. The acrylic was shaped into a rectangular profile which allowed the specimen to be securely clamped to the testing apparatus. A steel bar was also used in the clamping in order to further stabilize the specimen. The testing apparatus included an aluminum column upon which the bone specimen was clamped. This placed the bone sample in a cantilever testing mode. The aluminum column was screwed to a thick aluminum base which was c-clamped to a marble table base [Figure 4-1].

Each sample was positioned with the cranial surface of the radius up and the proximal end as the free end. The accelerometer was glued to the caudal surface at the free end. The impact hammer was used to lightly strike the bone at the free end [Figure 4-2].

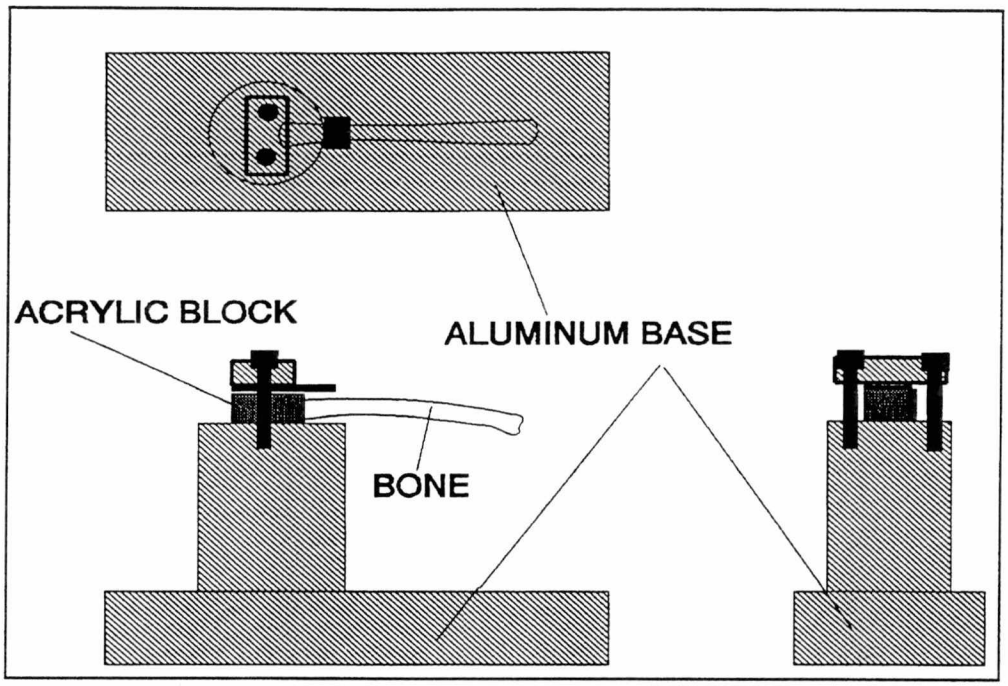


Figure 4-1. Fixturing apparatus for stabilizing bone samples for impact testing.

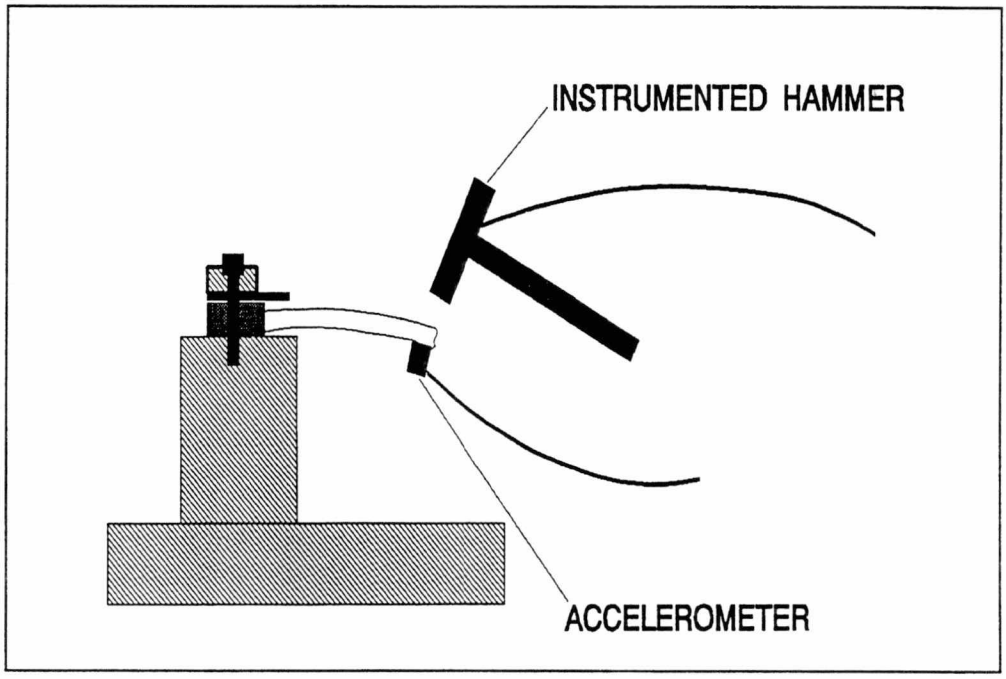


Figure 4-2. Schematic of the point of impact and the position of the accelerometer.

The impact hammer and accelerometer were connected to a model 3562 Hewlett Packard Dynamic Signal Analyzer, a small amplifier and a graphic plotter [Figure 4-3].

Following vibrational testing the acrylic block was removed from the bone with a chisel and mallet. This allowed quick and easy removal without damaging the specimen. Once the acrylic was removed the bone was then subjected to three point bending in an Instron testing machine from which load deformation curves were established for each bone.

## Data Collection and Processing

Data collection and processing involves transduction, preprocessing, postprocessing and data analysis. Transduction is the process of recording physical events as electronic

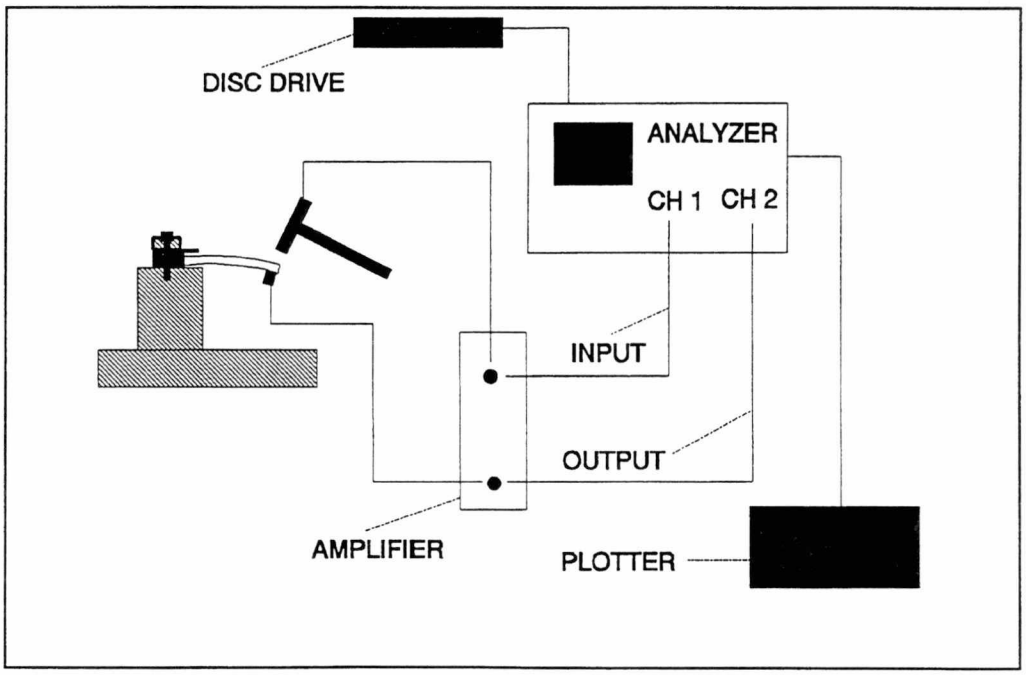


Figure 4-3. Schematic for data acquisition and processing.

signals. Preprocessing involves the amplification of these electronic signals. Postprocessing converts the analog signals to digital units of information. In the final step, the digitized information is analyzed and presented in graphical form for evaluation and comparison.

### *Transduction*

Physical parameters such as mechanical force, displacement, and acceleration involve a transfer of energy. A transducer is a specialized instrument that has the capability of converting this mechanical energy into electrical energy. From the different types of transducers available, the piezoelectric transducer was used in this study. A crystal with piezoelectric properties constitutes the energy conversion capability of these transducers. Crystalline structures have an organized arrangement of electrical charges on their surface. Mechanical energy delivered to the crystal causes deformation of its organized structure. This deformation redistributes electrical charges creating electrical energy in the form of a recordable signal. Once the initial event ceases, the crystal resumes its normal shape. It is then ready to respond to the next event.

### *Force Transducer*

The typical force transducer has the negatively charged surface of the piezoelectric crystals mounted to the casing. The positively charged surface is facing the positively charged surface of a paired crystal. The force transducer is positioned on the end of the

impact hammer. The force from the impact is passed through the transducer. The amount of force that passes through the crystals is dependent on the relative stiffness present in the direction of the applied force of both the crystals and the casing. Forces in transverse or angled directions to the orientation of the crystals can also induce electrical signals. These associated signals can complicate data processing. A small portion of the force recorded by the crystals is used in moving the mass of material present between the crystals and the test structure. In order to reduce this effect the softer end of the hammer is used to impact the test structure. In order to maximize signal input, a soft plastic tip was used in this study. The bone was struck in one position at the end of the radius just opposite the position of the accelerometer.

### *Accelerometer*

An accelerometer is also a transducer based on the generation of an electronic signal by a piezoelectric crystal. However, with the accelerometer, the relationship between actual acceleration and the recorded acceleration is indirect. The basic construction of an accelerometer is similar to the force transducer, but a seismic mass is added to the accelerometer. As a result of movement of the transducer, the force recorded by the crystals is actually the inertial force of the seismic mass which is also moving within the accelerometer itself. As a result, the mass of the accelerometer is critical to its sensitivity. The larger the mass of the accelerometer the better the sensitivity. However, large accelerometers can add a significant mass to the test structure thereby introducing inertial

forces that are not part of the original input. The accelerometer used in this study was a PCB 303A03 with a mass of 2 gm.

Attachment of the accelerometer to the specimen is also important in getting clean response data. This connection must be sufficiently rigid to allow for unaltered transmission of energy from the test specimen to the accelerometer. In this study, the accelerometer was secured to the bone with a cyanoacrylate adhesive. Cyanoacrylate is effective in adhesion to biologic tissue and was ideal for this test.

### *Preprocessing (Amplification)*

The test electronic signal is generally too small for processing thereby necessitating amplification. Undesirable stray electronic signals called "noise" can complicate the amplification process. Due to high impedance, piezoelectric transducers are susceptible to noise if the cable connecting the transducer to the amplifier is too long. Field effect transistors are incorporated in the transducer housing to help eliminate these noise signals. This requires that the direct current supply voltage is carried in the same wire as the test signal. This voltage can be much higher than the test signal, limiting amplification. To eliminate this problem, the system can be filtered with a "high-pass" filter. In addition to high-pass filtering, a "low-pass" filter can be used to eliminate high frequency signals that are not generated from the test specimen.

Once the signal has been generated and amplified, it must be processed or analyzed for presentation in a meaningful format. In this step of data analysis, the analog signal is

converted to a digital representation. Following digitalization the information is presented in its final format by the Hewlett-Packard 3562 Dynamic Signal Analyzer. The final format includes plotting of the frequency response, coherence, power spectrums, real and imaginary coefficients and the calculation of coefficients for damping. From these expressions parameter identification of natural frequency and damping is made.

### *Postprocessing (Analyzer Function)*

#### Analog to Digital Conversion

Amplitude determination is made through the use of an analog-digital converter (A-D converter) and a comparator. Test signals are analog in nature and in order to describe these signals mathematically they must be converted to a digital format. Using an analog-digital converter this is accomplished in a step-wise fashion by comparing the analog signal with a known reference voltage. Converters are rated from a three bit to a sixteen bit converter. Each bit is a switch and represents an incremental increase in reference voltage. When the incoming signal voltage reaches the converter, the comparator recognizes the difference between the input and reference voltage as a positive or negative numerical value. If the difference is positive, that is the input voltage is larger than the reference voltage, the next bit or switch is activated. This next bit has a higher reference voltage. The comparison is made again. This continues until the difference is negative, that is the input voltage is smaller than the reference voltage. The magnitude of the signal is read as the last reference

voltage that the difference was positive. The HP 3562A Dynamic Signal Analyzer has a 12 bit A-D converter. There is some deterioration of the signal as a result of this process but once the conversion is made there are no other sources for deterioration.

Analyzer Protocol

The Linear Resolution Mode was selected because it would give the most options for data presentation. In this mode the analyzer performs the FFT within a range of 0 - 100 kHz.

| Linear Resolution | | | | |
|---|---|---|---|---|
| MEASURE: | CHAN 1<br>Freq Resp | | CHAN 2<br>Freq Resp | |
| WINDOW: | CHAN 1<br>Force | WIDTH<br>14.0mS | CHAN 2<br>Expon | DECAY<br>20.0mS |
| AVERAGE: | TYPE<br>Stable | # AVGS<br>10 | OVERLAP<br>0% | TIME AVG<br>Off |
| FREQ: | CENTER<br>500 Hz | | SPAN<br>1.0kHz | BW<br>1.25 Hz |
| | REC LGTH<br>800mS | Δt<br>391μS | | |
| TRIGGER: | TYPE<br>Chan 1 | LEVEL<br>5.0mVpk | SLOPE<br>Pos | PREVIEW<br>Off |
| INPUT: | RANGE | ENG UNITS | COUPLING | DELAY |
| CH 1 | 35.5mVpk | 100mV/EU | AC (Flt) | 0.0 S |
| CH 2 | 892mVpk | 10.0mV/EU | AC (Flt) | 0.0 S |
| SOURCE: | TYPE<br>Off | | LEVEL<br>0.0 Vpk | OFFSET<br>0.0 Vpk |

Figure 4-4. Analyzer protocol for impact testing of all bone samples.

The following describes the major features of the selected analyzer protocol.

### *Measure*

Under Measure, "Frequency Response" was selected which gives both amplitude (gain) and phase shift information. Channel 1 was selected for the input signal from the impact hammer and Channel 2 for the output signal from the accelerometer.

### *Window*

Random vibration is sampled by the analyzer over a finite period of time. It is assumed that this finite sample is repeated over infinity. When these samples are connected together to describe the motion over infinity, considerable error can be introduced depending on what the data looks like at the ends of the sample period. The most accurate portion of the sample is in the center of the sample period. To improve the representation of the actual motion, a technique can be used to minimize the data at the ends of the sample period. The connecting of samples with zero data at the ends will preserve the essential character of the actual motion. This technique has been termed "windowing". Mathematically it involves the crossing of a known function with the test wave using the convolution theorem. This known function forces the data to approach zero at the limits of the sample time. For a transient signal such as impact, the problem is not as severe as for continuous input. However, by forcing the data to be maximized during the initial part of the sample time and minimized at the end of the time, a single unit step function is crossed with the actual recorded function. By forcing the input signals to zero by the end of the sample time, the

effect of contaminating signals can be canceled out. This unit step function is called the force window. The width of the force window was 14.0 ms.

The same problem can be associated with the output signal although the pattern of the output signal is different. The expected output is a decaying exponential. In order to ensure that the data within the sample time decays as expected, an exponential decaying function is crossed with the output data. Therefore the exponential window was selected for the accelerometer signal. The decay was selected at 20.0 ms.

### *Average*

Stable averaging was selected for this test. This type is a root mean square derived average and is the arithmetic mean of a selected number of tests; ie, it is a cumulative average. Therefore each test presented as a frequency response is actually a mean of 10 individual tests.

"Percent of Overlap" refers only to signals that cover the entire sample time. For such signals windowing influences the data at the ends of the sample period. In order to eliminate this data from the averaging process a percent of overlap is selected. For impact testing where the signal is transient and not continuous throughout the sample time, percent overlap is not necessary.

Time averaging was not selected because the data presentations desired such as frequency response, coherence and power spectrums are analyzed in the frequency domain. Time averaging is done only in the time domain.

### *Frequency*

The sampling rate, that is the points recorded per second, is critical for accurate representation of the true wave form being analyzed. If the frequency of the signal is high and the sampling rate is too slow, the frequency of the signal presented by the analyzer will be too low to be an accurate representation and therefore unsuitable for parameter estimation. This phenomenon is called "aliasing". Anti-aliasing filters are built in the analyzer to reduce the aliasing effect. However, if the setting of the maximum frequency is too low, the effectiveness of these filters is adversely affected. Also if the setting of the maximum frequency is too high, then frequency resolution is compromised.

The sampling rate is determined by the maximum frequency by using the Shannon Sampling Criteria:

$$f_s = 2(f_{\max})$$

The total time for the sample is determined by the number of points within a block which is already set within the analyzer. The total time for a sample is:

$$T = \frac{Points\ /\ block}{f_s}$$

Frequency resolution is determined by the assignment of maximum frequency. The frequency resolution is:

$$\Delta f = \frac{f_{\max}}{\frac{points\ /\ block}{2}}$$

The HP 3562A Dynamic Signal Analyzer presents 1024 points per block.

The maximum frequency selected for this study was 1.0 kHz. With this setting the analyzer set the record length at 800 mS and band width of 1.25 Hz and a delta t of 391 micro seconds. For the center frequency, 500 Hz was selected. The center frequency is a reference point used by the analyzer in various calculations.

### *Trigger*

Channel 1 was selected for the input signal. The minimum level for activation was selected to be 500 mV.

### *Input*

Input range is set so that the actual input signal is approximately one half of the set maximum input. Overrange input will distort the signal and as a result the analyzer will automatically refuse to accept such signals. The input maximum for channel 1 was 35.5 mV and for the output, channel 2 was 892 mV. "Engineering Units" was selected which allows for specific labeling such as G's for the force instead of volts.

AC coupling employs the use of a series capacitor to reduce direct current signals and drifts from adversely influencing input signals.

### *Data Analysis*

Frequency Response Function (Transfer Function)

The frequency response function, also referred to as the transfer function, is the ratio of the system's output to its input. While the data is obtained in the time domain, it is converted to the frequency domain through the application of the Fourier transform. The frequency response function contains both amplitude and phase information. The independent variable, frequency (Hz) is plotted on the horizontal axis while the dependent variable, magnitude (g's/lb force) is plotted on the vertical axis. From this curve, natural frequency and damping parameters can be approximated by selecting resonant frequency peaks.

The analyzer computes the Fourier coefficients in order to create the response curve. These coefficients constitute the mean square value of the individual harmonic present. The mean square value is made up of individual contributions in each frequency interval. These contributions are the coefficients multiplied by their complex conjugates. This square value is called the power spectrum. When all the input coefficients are multiplied by their complex conjugates, an input power spectrum is obtained. In this power spectrum, phase information is eliminated. Phase information can be retained by computing a cross spectrum. In this case, the coefficients of the input are multiplied by the complex conjugates of the output

spectrum. The analyzer utilizes these averaging techniques to create the frequency response function:

$$H_f = \frac{G_{XY}}{G_{XX}}$$

where:

$$H_f = Transfer\ Function$$
$$G_{XY} = Cross\ Spectrum$$
$$G_{XX} = Input\ Power\ Spectrum$$

The choice of frequency interval will affect the power spectrum and the mean square value. To reduce this influence the power spectral data are normalized by dividing the power spectrum by the frequency interval. This value is called the power spectrum density and is more consistent and reflective of the actual condition.

Power Spectrums

To observe the magnitude or amplitude changes without the influence of phase shifts, power spectrums were produced. For random signals, phase information is not as useful as for periodic signals. Power spectrums for input (Power Spectrum 1) and output (Power Spectrum 2) were produced separately by multiplying the coefficient of the respective signal by its complex conjugate.

Coherence

When depending on a ratio of output to input, it is critical to make sure that all the output is due to the input. With impact testing, the probability of noise contamination of the output is high. In order to identify the occurrence of noise contamination, an additional function called coherence is produced along with the frequency function. The coherence function is defined as:

$$\gamma^2 = \frac{G_{XY} G_{XY}^{\star}}{G_{XX} G_{YY}}$$

where

$$G_{XY} = \textit{Cross Spectrum}$$
$$G_{XY}^{\star} = \textit{Cross Spectrum Conjugate}$$
$$G_{XX} = \textit{Input Power Spectrum}$$
$$G_{YY} = \textit{Output Power Spectrum}$$

The coherence value is a dimensionless quantity that ranges between 0 and 1. A value of 1 indicates that all of the response is due to the input, while a value of zero indicates that none of the response is due to the input.

## Real and Imaginary Plots

To evaluate the reliability of a frequency peak as representative of a true natural frequency, plots of the behavior of the real and imaginary coefficients is helpful. At resonance the real coefficients should tend to zero while the imaginary coefficients tend to maximum.

## Damping

In addition to natural frequency, damping is also derived from the frequency response curve. Once a maximum peak value is selected, the analyzer automatically bands the curve to a width of 20 points on either side of the peak. A single degree of freedom curve fit is applied to that portion of the curve including the peak. From this curve, the real part (D value) and the imaginary part (F value) of the complex pole at resonance is calculated[1]. From these two values a damping value is computed[2]:

$$\zeta = \frac{D}{\sqrt{D^2+F^2}}$$

---

[1]Smith B. Personal Communication. Hewlett-Packard Co., Everett, WA, 1998.

[2]De Arbogast. Personal Communication. Hewlett-Packard Co., Everett, WA, 1998.

Due to the fact that some of the "D" values were negative the entire expression was squared. The result was multiplied by 100 to obtain a percent of damping:

$$\%\ of\ damping = [\sqrt{\frac{D^2}{D^2+F^2}}]\ 100$$

As the resonant frequency peak becomes sharper the above damping value approaches zero. In lightly damped systems nearly all the energy is used in producing amplitude and displacement. In such systems resonant frequency peaks will be high and sharp in contour. In heavily damped systems much of the energy is lost reducing amplitude and deflection. Frequency peaks in these systems are low and spread out. The behavior of the above damping value is consistent with the expected influence of damping.

## Statistical Analysis[3]

From the Instron testing data, values for fracture callus stiffness were obtained from the load deformation curves and compared statistically. The slope of the linear portion of the curve will give a "stiffness value". A linear region of the load deformation curve was selected for computation of the slope. The ultimate strength was obtained from the load deformation curve at the point of structural failure.

---

[3]Quattropro version 8, 1997

From the vibration testing data, the natural frequency values were obtained directly from the peak of the response curve. The damping values were obtained from a curve fit of the resonant frequency peak. To determine if natural frequency or damping were different between the intact and ostectomized specimens a paired t-test was applied. To determine if natural frequency or damping were different among the treatment groups a one way analysis of variance was applied. Linear regression was done to see if the changes in the vibration parameters correlated positively with the three point bending parameters.

# CHAPTER V

# RESULTS

## Natural Frequency

Frequency response curves were obtained for each bone specimen. In the linear resolution mode the ordinate axis records the magnitude of the transfer function in units of g's/lb force and the abscissa records the frequency in Hz. In conjunction with the frequency response curve, a coherence plot is displayed. From the frequency response curve, the highest resonant frequency peak is selected as representative of the first mode of bending. Results are listed in Table 5-1.

Load deformation curves were established for each specimen by three point bending. From these curves, the linear region was evaluated for slope which gave an assessment for the stiffness of the fracture callus. Also the ultimate load at failure was determined for each specimen. Results are listed in Table 5-2.

The natural frequencies of the intact bones were significantly higher than those of the ostectomized bones as a paired t-test was highly significant at $p < 0.05$. One way analysis of variance was also significant at $p = 0.003$. Therefore the natural frequency data obtained in this study were significantly different among the treatment groups. However, there does not appear to be a significant difference between treatment group 3 and 6. Also linear regression between the treatment groups and the mean frequency values of the treatment

**Table 5-1. NATURAL FREQUENCY AND PERCENT DAMPING**

| | | Ostectomy | Ostectomy | Intact | Intact |
|---|---|---|---|---|---|
| Dog # | Group | Nat Freq Hz | % Damp | Nat Freq Hz | % Damp |
| C97153 | 0 | 57.5 | 49.48 | 205.0 | 1.87 |
| C97156 | 0 | 61.2 | 3.32 | 143.7 | 8.39 |
| C97161 | 0 | 147.5 | 3.77 | 408.7 | 3.89 |
| C97176 | 0 | 45.0 | 39.62 | 251.2 | 2.44 |
| C97154 | 3 | 146.2 | 2.47 | 257.5 | 3.97 |
| C97158 | 3 | 145.7 | 6.04 | 245.0 | 1.25 |
| C97163 | 3 | 152.5 | 2.04 | 306.2 | 3.11 |
| C97167 | 3 | 150.0 | 2.06 | 271.2 | 4.60 |
| C97152 | 6 | 122.5 | 3.38 | 258.7 | 3.84 |
| C97159 | 6 | 150.0 | 1.66 | 200.0 | 6.20 |
| C97173 | 6 | 146.2 | 5.03 | 318.7 | 4.32 |
| C97177 | 6 | 158.7 | 3.71 | 237.5 | 5.19 |
| C97155 | 12 | 206.2 | 5.89 | 233.7 | 5.52 |
| C97157 | 12 | 238.7 | 5.75 | 290.0 | 4.63 |
| C97172 | 12 | 290.0 | 1.22 | 290.0 | 1.33 |
| C97178 | 12 | 140.0 | 12.59 | 237.5 | 11.3 |

**Table 5-2. ULTIMATE LOAD AT FAILURE AND STIFFNESS**

| | | Ostectomy | Ostectomy | Intact | Intact |
|---|---|---|---|---|---|
| Dog # | Group | Ult Fail<br>lb | Stiff<br>lb/in | Ult Fail<br>lb | Stiff<br>lb/in |
| C97153 | 0 | 1.1 | 10.0 | 210.0 | 3100.0 |
| C97156 | 0 | 22.5 | 50.0 | 188.0 | 2500.0 |
| C97161 | 0 | 28.5 | 210.0 | 257.0 | 2500.0 |
| C97176 | 0 | 4.8 | 15.0 | 240.0 | 4000.0 |
| C97154 | 3 | 17.5 | 130.0 | 190.0 | 2800.0 |
| C97158 | 3 | 24.0 | 200.0 | 228.0 | 3750.0 |
| C97163 | 3 | 35.5 | 300.0 | 248.0 | 4750.0 |
| C97167 | 3 | 28.0 | 275.0 | 186.0 | 3250.0 |
| C97152 | 6 | 51.6 | 700.0 | 280.0 | 2500.0 |
| C97159 | 6 | 44.0 | 300.0 | 246.0 | 5100.0 |
| C97173 | 6 | 41.7 | 425.0 | 248.0 | 4250.0 |
| C97177 | 6 | 55.0 | 600.0 | 200.0 | 3500.0 |
| C97155 | 12 | 78.0 | 1150.0 | 260.0 | 3250.0 |
| C97157 | 12 | 69.0 | 950.0 | 273.0 | 3500.0 |
| C97172 | 12 | 70.0 | 200.0 | 198.0 | 2750.0 |
| C97178 | 12 | 61.3 | 450.0 | 169.0 | 2550.0 |

groups showed a 95% ($r^2$=0.95) positive correlation. The natural frequency data behaved as expected in that as fracture healing improved with treatment by somatotropin, the natural frequency increased in value [Figure 5-1].

Also by regression analysis the correlation between the changes in ultimate strength and natural frequencies was good at an 80% ($r^2$=0.80) positive correlation. The correlation between stiffness and natural frequency was not as good at a 53% ($r^2$=0.53) positive correlation.

## Damping

From the frequency response curves the percent of damping was calculated as described in the Materials and Methods section. The results of the data are presented in Table 4-1.

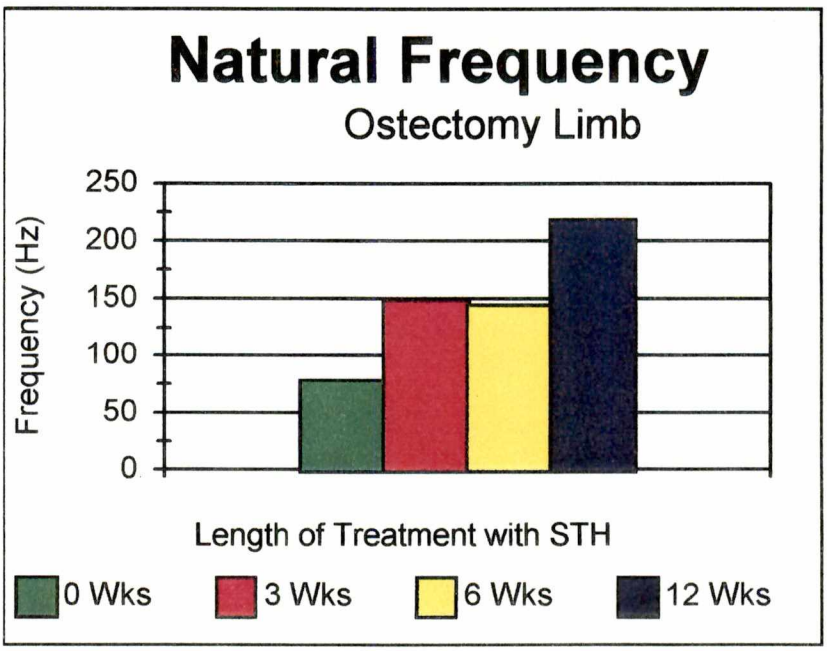


Figure 5-1. The natural frequency showed a gradual increase in value linearly corresponding to the increasing length of treatment with somatotropin.

A paired t-test was applied to the percent damping data between ostectomized and intact bones was not significant. There was considerable variance within the control group that prevented the damping data from being statistically significant.

One way analysis of variance was also applied to the percent damping data. There were no significant differences between the treatment groups at $p = 0.09$. When viewing the trend in damping values, there appears to be more damping in those specimens not treated with somatotropin [Figure 5-2].

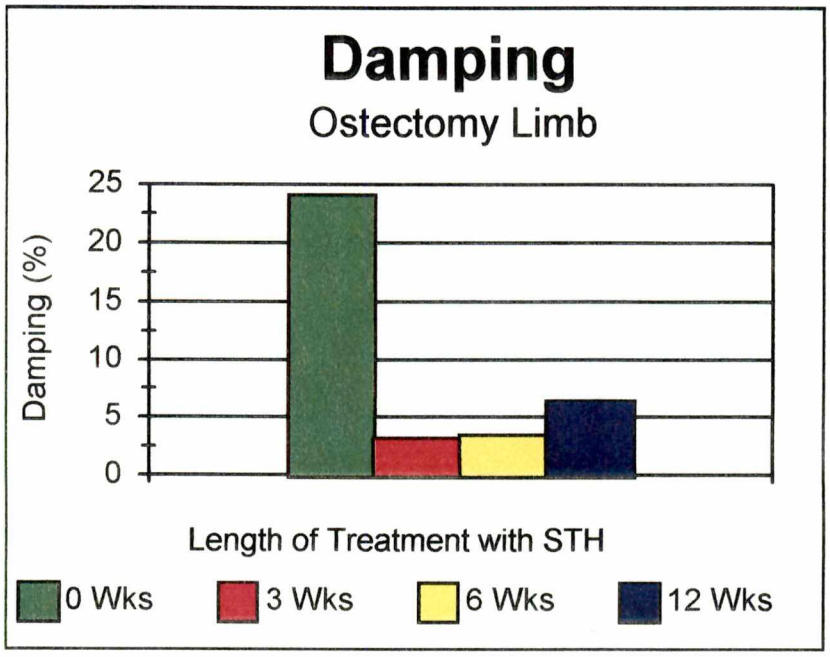


Figure 5-2. Damping as expected is high in the control group, but because of wide variance within this group there were no significant differences between the groups.

However there was too much variance within the control group to make these results statistically significant.

Linear regression found a negative correlation between the changes in stiffness and ultimate strength and the changes in damping.

# CHAPTER VI

# DISCUSSION

## Bone Healing

The four biologic phases of bone healing are the inflammatory, soft callus, hard callus, and remodeling phases (Brown et al, 1993). The inflammatory phase is the initial process following fracture. In this phase, the soft tissues surrounding the fractured bone are stimulated to orchestrate a clean up and to initiate the healing process. This process is mediated by cells that are stimulated by biochemical substances released by the injured tissue. The inflammatory cells are injured local cells, invading mast cells, leukocytes, macrophages, and lymphocytes. Pluripotential cells from the periosteum, endosteum and perivascular tissues become available for differentiation into cells capable of forming connective tissue. Some endocrine compounds that are increased are parathormone and calcitonin. Vitamin D metabolites and alkaline phosphatase are also found in increasing amounts. The hematoma, which is clotted blood present in the fracture site, serves as a source of platelets which in turn releases cell mediators and growth factors. Among these compounds, platelet-derived growth factor, epidermal growth factor and transforming growth factor beta will stimulate callus formation. Hyaluronate found in healing fractures promotes migration and proliferation of mesenchymal and endothelial cells. Macrophages, important in the debridement and the clean up process also promote fibroplasia. From these

macrophages, interleukin-1 causes systemic signs of inflammation such as fever and in the other nonfractured bones, an increased activity of the bone marrow and osteoclasts. Also interleukin-1 stimulates the release of prostaglandin E-2 which promotes bone resorption. As a result of this activity, new capillary blood vessels begin to form in conjunction with the growth of tender collagen fibers crossing the fracture gap. These new tissues form and migrate on a fibrin meshwork present in the organizing hematoma. In this initial phase, the fracture is unstable and motion is prevalent, however, the healing tissues are very elastic allowing 100% strain before rupture.

Phase two is recognizable at approximately 2-3 weeks following the fracture. This phase is referred to as the soft callus phase. In this stage, the granulation tissue that initially formed between the fragments is being replaced by fibrocartilage, a more rigid tissue but still pliable and somewhat elastic. The conversion to this tissue type occurs initially at the periphery of the callus and proceeds toward the center. Osteoclasts that have moved into the area are resorbing the dead bone. Osteocytes and endosteal cells differentiate into osteoblasts and chondroblasts which then begin the actual formation of cartilage and bone. The chondrocytes come from pluripotential mesenchymal cells. Osteoblasts, the bone producing cells, can originate from pluripotent mesenchymal cells present in all connective tissue and from bone marrow and endosteum. These cells are also stimulated by the same mediators listed above.

The next phase is dominated by the formation of hard callus and is characterized by the mineralization and stiffening of the callus. Similar to the pattern of growth of the soft

tissue callus, the mineralization process begins at the periphery and progresses toward the center. Once the bony bridge is complete, motion of bone fragments is eliminated.

Once the fracture has been stabilized by the hard callus, the phase of remodeling takes place. In this phase the woven bone that was previously formed is removed and replaced by more organized lamellar bone that is complete with Haversian systems. This process is responsive to the mechanical stress that is delivered to the bone in that compression stimulates bone formation. The remodeling phase removes in a gradual and slow process the hard callus that originally united the fracture and replaces it with a more normal organized cortex surrounding a reconstituted marrow. This process can proceed for years following the fracture.

## Growth Hormone Effects

Somatotropin or pituitary growth hormone is produced and released from the anterior pituitary gland and is most active in the growing animal. Once the animal reaches maturity, especially when aged, the levels of somatotropin decrease. This hormone is responsible for stimulating many of the tissues of the body to grow and develop. The principal interest here is in its effect on bone production.

Somatotropin has both a direct and indirect effect on bone production. As previously mentioned, insulin-like growth factor I is active in fracture healing. Somatotropin functions in increasing the levels of insulin-like growth factor I and bone morphogenic protein.

Somatotropin is also known to enhance endochondral ossification of the growth plate by stimulating cartilage cells (Best and Taylor, 1966).

Previous studies have had difficulty in showing a positive effect with the administration of somatotropin. This is due in part to the fact that species specific hormones are more effective. Species specific somatotropin was not available in earlier investigations. In this present study, species specific recombinant canine somatotropin was used to stimulate fracture healing. However, the primary objective was to determine the most ideal duration of treatment.

It has been demonstrated that recombinant canine growth hormone enhances fracture callus production in a canine radial ostectomy model (Millis et al, 1998). In that study both the ultimate strength and stiffness of the fracture callus was significantly better in the treated vs the non-treated dogs. The mean ultimate strength was three times higher in the treated dogs and the mean stiffness was five times greater in the treated dogs. The callus of the treated dog was more mineralized and larger in size than the non-treated dog.

## Nonunion Fracture Model

A fracture that does not heal within an expected time or quits showing evidence of healing is called a delayed or nonunion fracture. A common cause of this type of complication is excessive motion at the fracture site. If the interfragmentary strain exceeds the tolerable limits of the bridging tissue, the body ceases in its effort to heal the gap. As a result of repeated instability, the body adapts to instability rather than achieving stability.

Another factor that contributes to a reduction of healing effort is the width of the space between fragments. It is more difficult for a fracture callus to form when large gaps are present between bone fragments. This factor coupled with instability ensures difficult healing. A partial radial ostectomy of a 3 mm gap has been documented as a reliable model for creating a delayed or nonunion fracture in the dog (Heckman et al, 1991; Volpon, 1994).

In this model the companion bone, the ulna, remains intact. This reduces the morbidity associated with a partial radial ostectomy because limited function of the leg is possible even without external or internal support. Allowing these dogs to ambulate without casts or splints also enhances the motion at the ostectomy site facilitating the production of a poor healing event. In this model, with the mechanical factors stacked against normal healing, the influence of the biological factor of somatotropin would be evident.

## Callus Nonhomogeneity and Geometry

When evaluating a biological structure such as a healing bone, there are several factors that can contribute to difficulties in measurements. In the analysis of beams, homogeneity of the material composition of the beam is required in order to use Hooke's law of linear elasticity. However, a fracture callus is more like a composite beam and therefore does not necessarily respond in a linear fashion. The callus contains several tissue types, all with different mechanical behaviors. As the callus develops, these tissue types change in their concentration and arrangement within the callus. A one week callus may contain a

disorganized arrangement of soft collagen and fibrin while a twelve week callus will contain stiff bony elements in combination with more elastic cartilaginous and fibrous regions.

Along with the nonhomogeneity of the callus is the asymmetry of its cross sectional geometry. In basic beam theory, the beam is assumed to be symmetric with respect to the plane of bending. The cross section of a developing callus is not symmetric and it is a difficult task to determine accurate area moments of inertia.

All these factors contribute to the nonlinearity of the healing bone as a test structure. Testing effectiveness and reliability will depend on the consideration of this inherent nonlinearity.

## Natural Frequency

### *Trial Samples*

Steel Bar

In order to verify that this test protocol was reasonable, a rectangular steel bar with a first natural frequency that could be calculated from known material properties was impact tested. The first natural frequency obtained from the impact test should favorably compare with the calculated value.

As expected for a lightly damped structure the frequency response curve for the steel bar yielded a clear and definite resonant frequency peak at 1.415 kHz This peak was characterized as a sharp, smooth, narrow curve. An accompanying coherence plot showed a high degree of correlation between input and output energies indicating that the test was valid [Figure 6-1].

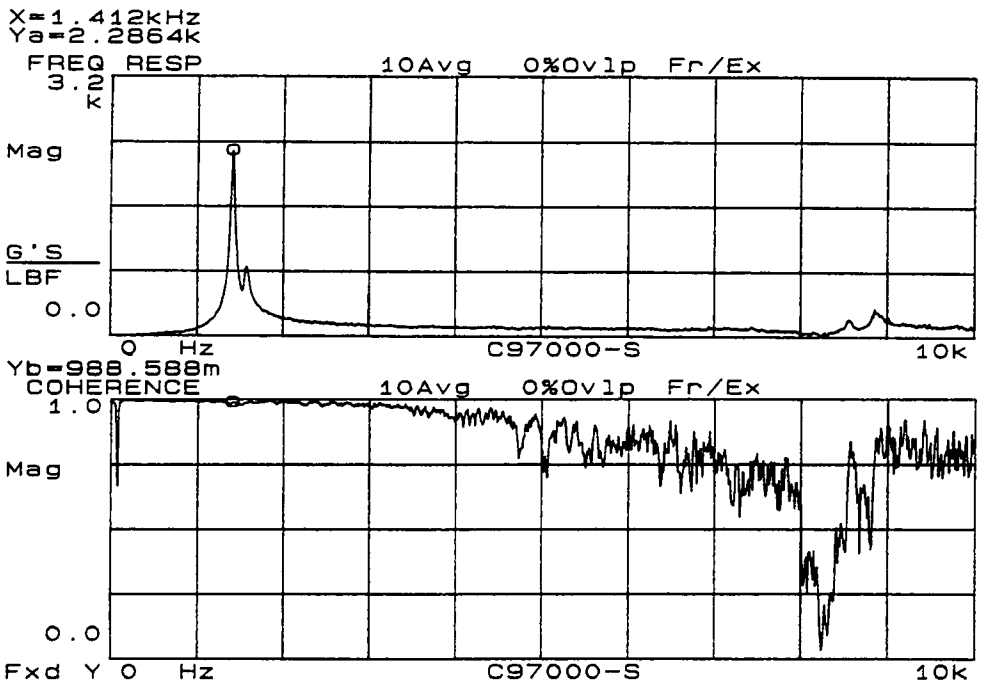


Figure 6-1. Frequency response curve and coherence for the impact test of a rectangular steel bar.

Consider the following expression for the deflection of an end loaded beam (Gere and Timoshenko, 1984):

$$v = \frac{PL^3}{3EI}$$

and solve for the end load P:

$$P = \frac{3EI}{L^3}v$$

The above expression states that the force "P" is proportional to the deflection "v". This is similar to the relationship between a spring force and the change in length of the spring. Therefore, the proportionality constant for the end loaded cantilever beam is (Blevins, 1979):

$$k = \frac{3EI}{L^3}$$

A reasonable approximation for the first natural frequency of the steel bar can be obtained by substituting the above expression for "k" into the basic expression for the natural frequency:

$$\omega_n = \sqrt{\frac{k}{m}} = \sqrt{\frac{3EI}{L^3 m}}$$

For this rectangular steel bar:

$$E\ (elastic\ modulus,\ steel) = 29{,}000\ lb/inch^2$$
$$b\ (width) = 1.11\ inch$$
$$h\ (height) = 0.370\ inch$$
$$l\ (length) = 2.299\ inch$$
$$m\ (mass) = 0.00069\ lb\ \sec^2/inch$$

And for the area moment of inertia:

$$I = \frac{bh^3}{12}$$

The calculated natural frequency was 1.1 kHz. This favorably compared with the experimentally derived natural frequency of 1.4 kHz.

The input energy for the steel bar as displayed in power spectrum 1, was sharp and pure with no additional input energies other than the impact. Likewise the output energy corresponds well with the input. It was clear, therefore, that there were no other sources of excitation or response to contaminate test results [Figure 6-2].

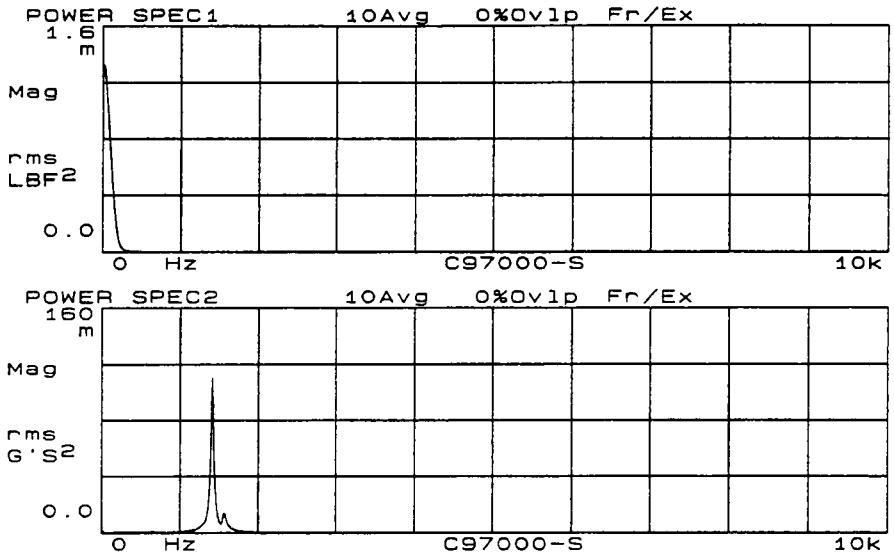


Figure 6-2. Input power spectrum 1 and output power spectrum 2 for the rectangular steel bar.

In comparing the performance of the real vs imaginary coefficients it can be seen that as the imaginary coefficient reaches maximum, the real coefficient approaches zero, which is consistent with a resonant frequency [Figure 6-3].

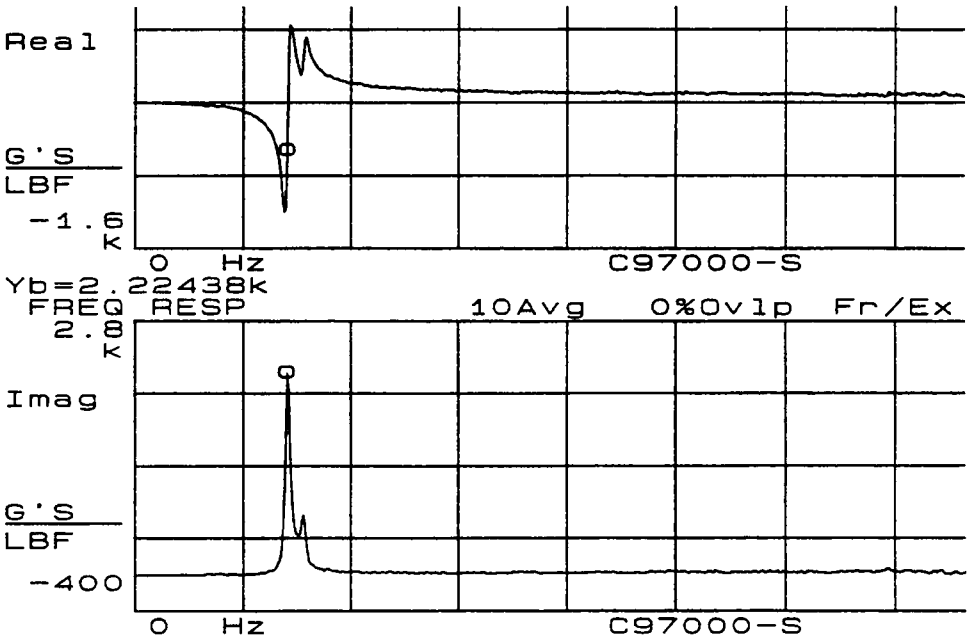


Figure 6-3. Real and imaginary coefficients for the impact test of the rectangular steel bar.

The frequency range for testing the canine bones was from 0 - 1000 Hz. The frequency response curve for the steel bar was reproduced within this frequency range to examine for any resonance that could be due to fixture vibration. However the curve was smooth with no peaks especially in the range from 0 - 500 Hz. All of the bone samples in this study had the first natural frequency inside this range [Figure 6-4].

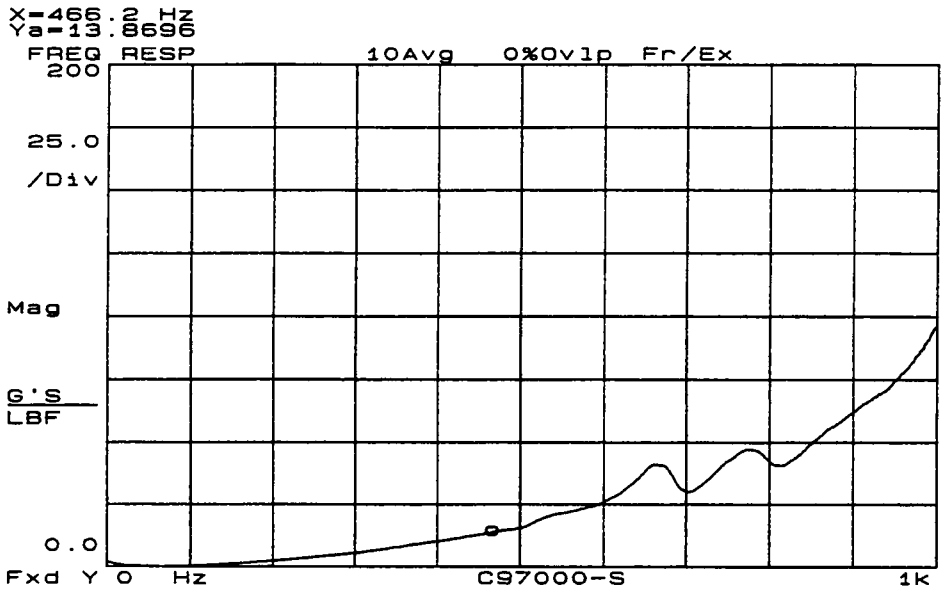


Figure 6-4. Between 0 and approximately 500 Hz, there are no resonant frequency peaks in this frequency response curve for the steel bar.

Trial Intact Dry Bone

An intact dried trial bone specimen was also tested and compared to the steel bar results. In contrast to the steel bar, on the frequency response curve, the first frequency peak was notched. Associated with the notch was a low coherence value. This indicates a contaminate signal has interfered with the response [Figure 6-5].

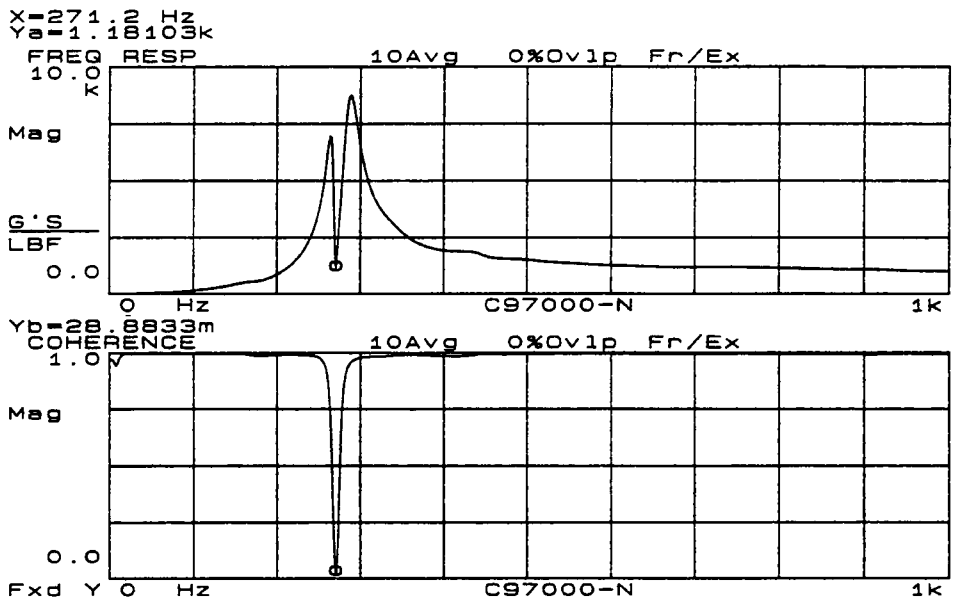


Figure 6-5. A severe drop in coherence is associated with this frequency response curve for the trial intact dry bone specimen.

The power spectral curves corroborate the existence of additional sources of output signal generation. The input, power spectrum 1, was a clean smooth curve representing an isolated excitation energy coming from the impact hammer. However, the output, power spectrum 2, displayed several small peaks in association with the primary peak [Figure 6-6].

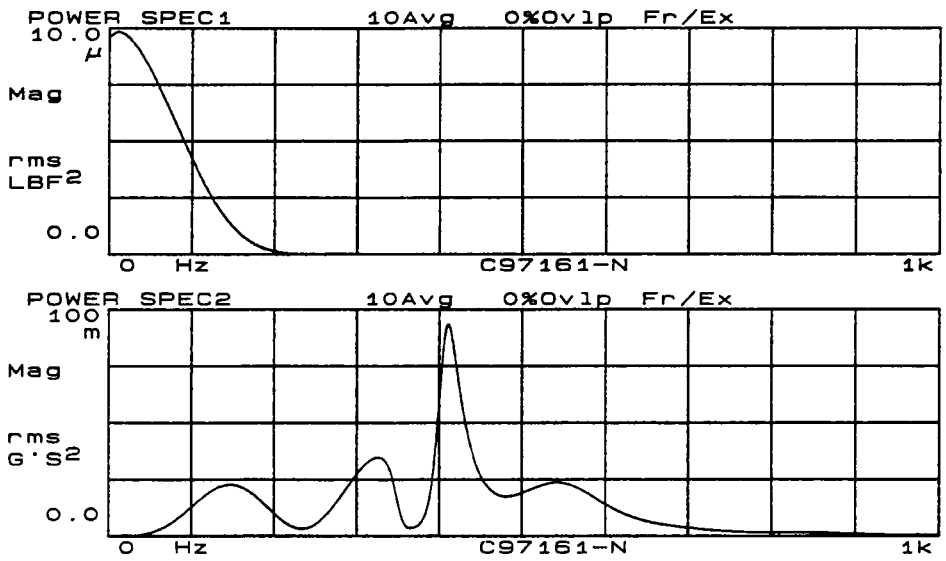


Figure 6-6. Power spectrum 2 shows four small peaks in addition to the single large output peak.

These smaller peaks represented other sources of response signals that were not coming from the impact hammer. The origin of these signals could be fixture vibrations or nonlinearities within the bone or the motion of the bone in an additional plane such as the transverse plane or possibly rotary motion. All fixture set ups for the bone specimens included an acrylic setting of the bone. When the steel bar was tested the acrylic fixture was not included. Thus

motion present between the acrylic and the aluminum and steel clamp or between the acrylic and bone could have contributed to the response.

In addition to the above effects, a mass effect of the accelerometer, while not a problem with the steel, could be a source of additional response energy. The bone samples in this study ranged in mass from 11 to 24 gm while the accelerometer mass was 2 gm. Since bone is more highly damped and not as stiff as steel, its deflections were larger than for steel. Large deflections could have also influenced the clarity of the response.

For this dry intact bone the coordination of real vs imaginary coefficients is very close to what would be expected at a resonant frequency [Figure 6-7].

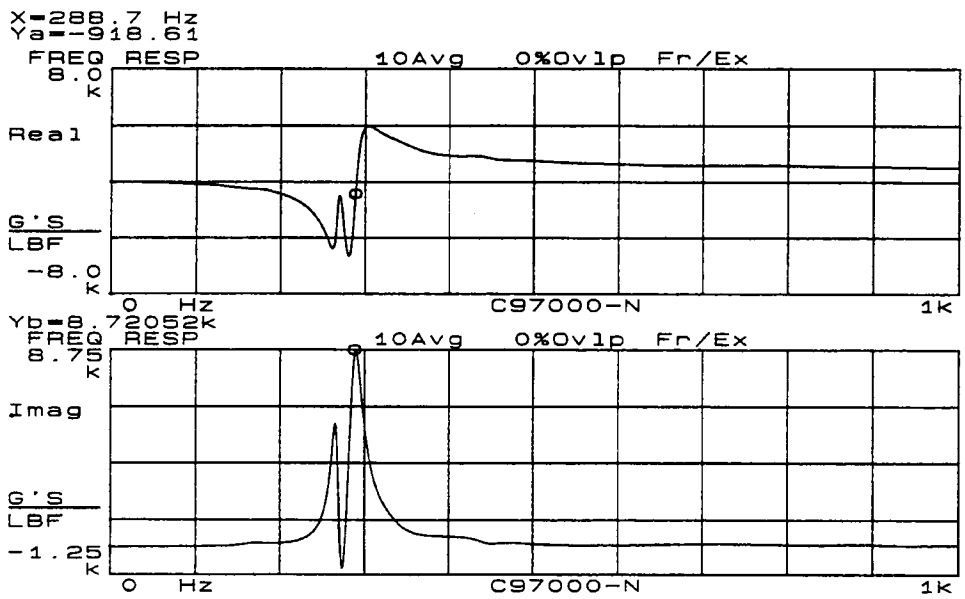


Figure 6-7. In these plots from the trial intact dry bone specimen, the maximum imaginary coefficient value corresponds with a near zero value for the real coefficient.

Therefore, in spite of the notched peak, the resonant frequency identified in this test most likely represents the first mode of vibration. Until the stray signal causing the notch is identified and removed, this test could not be used to determine an actual natural frequency in bone.

Trial Taped Dry Bone

A third trial sample tested was a dry sample of the radius that was cut and taped together to simulate a poor healing callus. The frequency response curve showed a smooth curve with no notch as was seen in the intact bone [Figure 6-8].

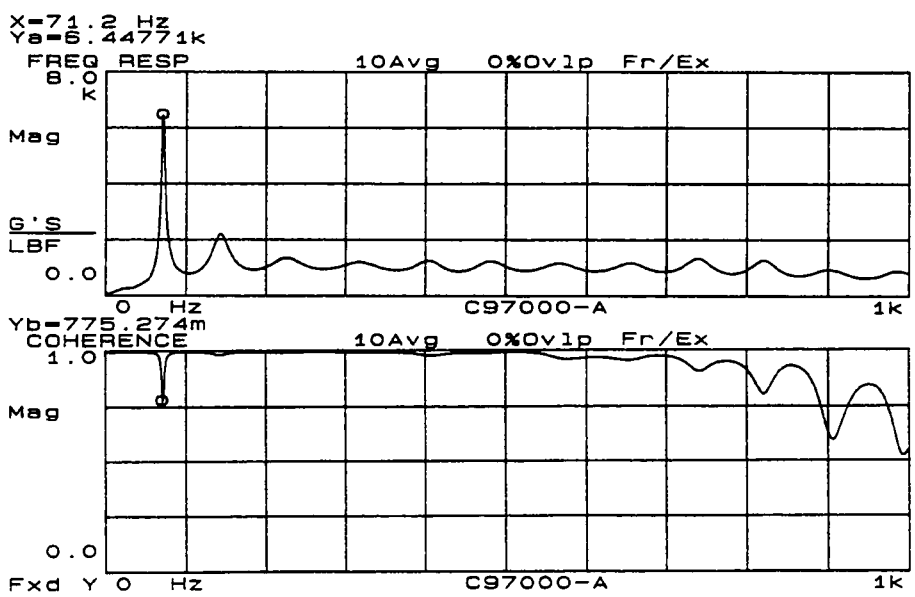


Figure 6-8. In this frequency response curve of the trial taped bone specimen, multiple smaller peaks are present throughout the frequency range (0 - 1 kHz).

Although the resonant peak is smooth, the coherence does drop but remains acceptable at a value above 0.5.

There were some unique differences in the frequency response curve associated with the taped bone. Following the initial peak there were additional small wide peaks. The possibility arose as to whether these additional peaks were other modes of vibration elicited in the unstable specimen. In conjunction with these differences both power spectral curves displayed additional peaks [Figure 6-9].

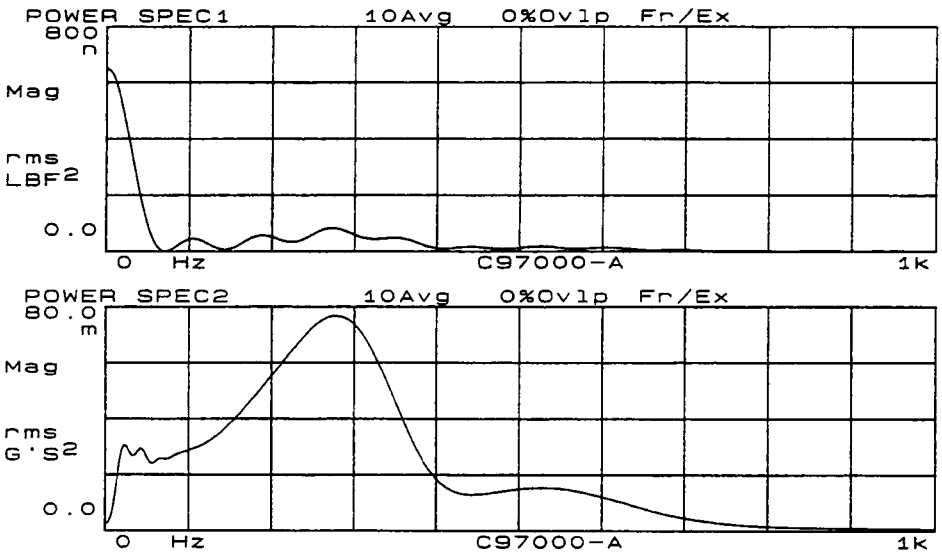


Figure 6-9. In the trial taped dry bone specimen, both power spectral curves show additional peaks indicating the presence of additional input and output energies.

In power spectrum 1 (input spectrum) there are additional peaks following the peak representing the initial impact. These peaks indicate other sources of excitation. Due to the severe instability of the taped bone, the delivered impact was so soft that the hammer and specimen may have had repeated contact causing additional sources of input energy. In power spectrum 2 (output spectrum) also had several additional peaks indicating additional

response signals. It is possible that with the unstable bone, the original single degree of freedom system become a two degree of freedom system such that the two fragments of the bone may be moving independently of each other in a manner that one fragment conjoins the other delivering additional output energies.

### *Experimental Samples*

#### Intact Bone Specimens

The nonostectomized intact bones behaved in a similar fashion to the dry intact trial specimen. The resonant frequency peaks corresponding to the first mode were notched in 11 out of 16 samples tested. Although a drop in coherence occurred with the notch, only in one case was the slump in coherence severe, ie when it came close to zero [Figure 6-10].

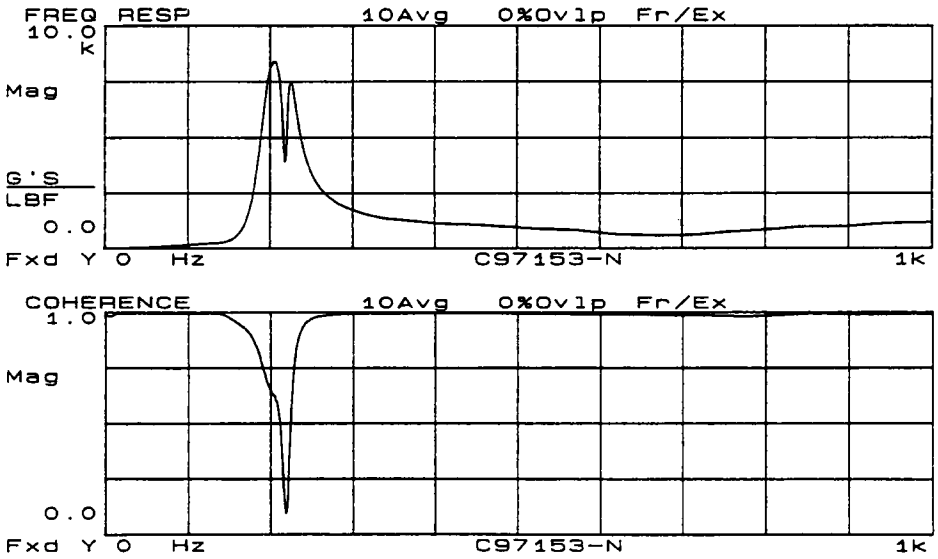


Figure 6-10. The resonant frequency peaks of this intact experimental sample from the control group shows a notch with a severe drop in coherence.

Although it was not determined in the course of the testing as to the source of the notched frequency peak, two possibilities could be considered. First, a response frequency emanating from the test structure itself could have resulted in a drop in coherence. In the steel bar trial, the response was examined in the frequency range of interest and no resonant peaks were seen. However, the acrylic fixture holding the bone was not part of the steel bar test. As a result the acrylic fixture was suspect in contributing to a contaminated response, such that motion between the acrylic and bone was possible. Second, motion of the bone sample in planes other than the primary bending plane could have contributed to the drop in coherence. The fact that there were 5 samples that did not exhibit a notched resonant peak supports the possibility that a fixturing problem between the acrylic and bone is the most likely possibility [Figure 6-11].

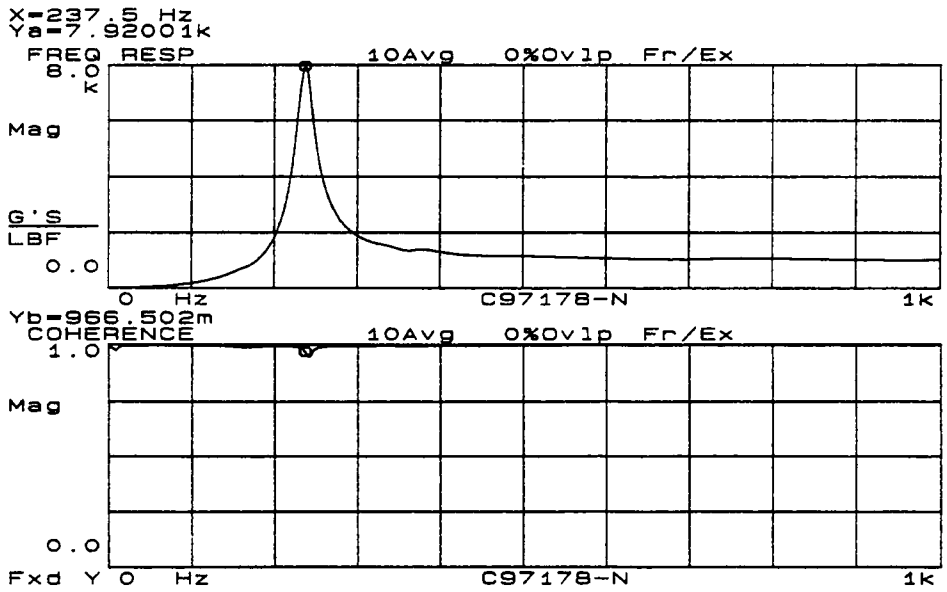


Figure 6-11. An example of an intact specimen with a clean resonant peak and good coherence.

The power spectral curves in all intact bone specimens were similar to the dry trial sample. The input power spectral curve was clean while the output had several additional peaks which represents multiple sources of output energy. Inherent nonlinearities within the bone could have been the source of these additional signals. Bone is a composite structure containing hard calcium hydroxyapatite crystals, softer collagen fibers, cells, fat, and water. All of these tissues respond differently and are not in themselves linearly elastic. Also in view of the bone's composite structure there is more damping which could have reduced the intensity of the desired response allowing other sources to contaminate the desired response signal. The correlation of the real vs imaginary plots was relatively good for the intact bones.

In spite of the above problems, the natural frequencies determined did not exhibit a statistically significant difference among the intact bones from any of the groups. This finding correlated well with the three point bending data which also showed no significant differences in the ultimate load to failure and stiffness in the intact bones. Although the natural frequencies obtained in this study behave in general as expected, the problems mentioned above would make determination of actual natural frequencies difficult.

Ostectomized Bones

The ostectomy group exhibited similar patterns to the taped bone specimen but as the callus developed under the influence of somatotropin, the testing profiles changed to parallel those of the trial dry intact bone specimen.

*Control Group*

The control group, which did not receive somatotropin, had the weakest callus and the poorest stiffness values when tested in 3 point bending. The frequency response curves showed a smooth but wide resonant peak followed by a series of smaller similar peaks at fairly regular intervals [Figure 6-12].

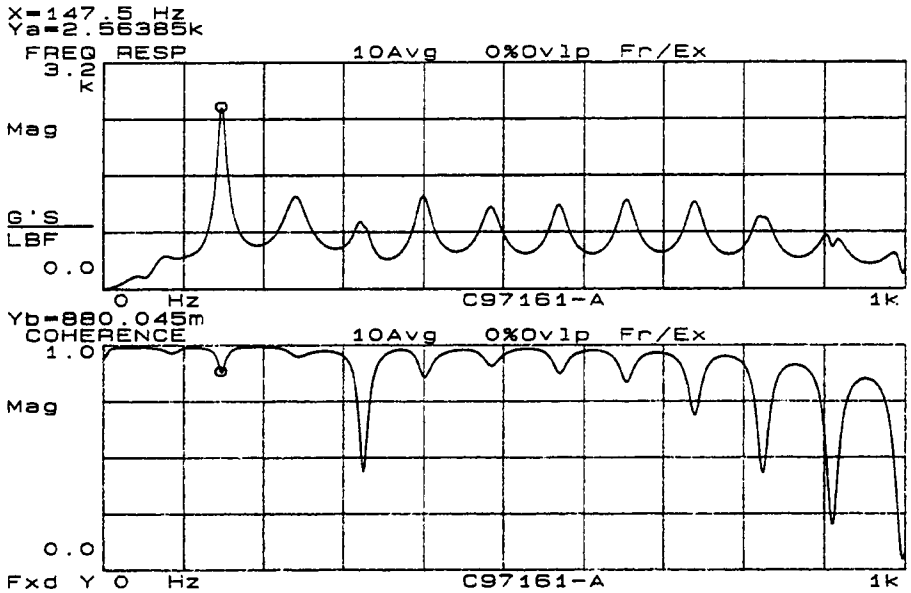


Figure 6-12. The frequency response curve from this ostectomized control specimen clearly demonstrates multiple resonant peaks throughout the frequency range (0 - 1 kHz).

Coherence remained at a high level and did not deteriorate until three quarters of the way through the frequency span. This would indicate that most of these peaks were due to the input signal. The principal difference between the control group and the others was the presence of a very unstable callus. The multiple peaks in the frequency response curve may have represented additional modes of vibration. The finding of good correlation of the behavior of the real and imaginary coefficients along with the high coherence supports the

conclusion that these peaks did represent resonant frequencies at corresponding modes of vibration. The origin of these additional peaks may be due to the fact that the unstable bone was acting as a two degree of freedom system with the two fragments moving and responding differently from each other.

The power spectrum from this group paralleled that of the taped sample [Figure 6-13].

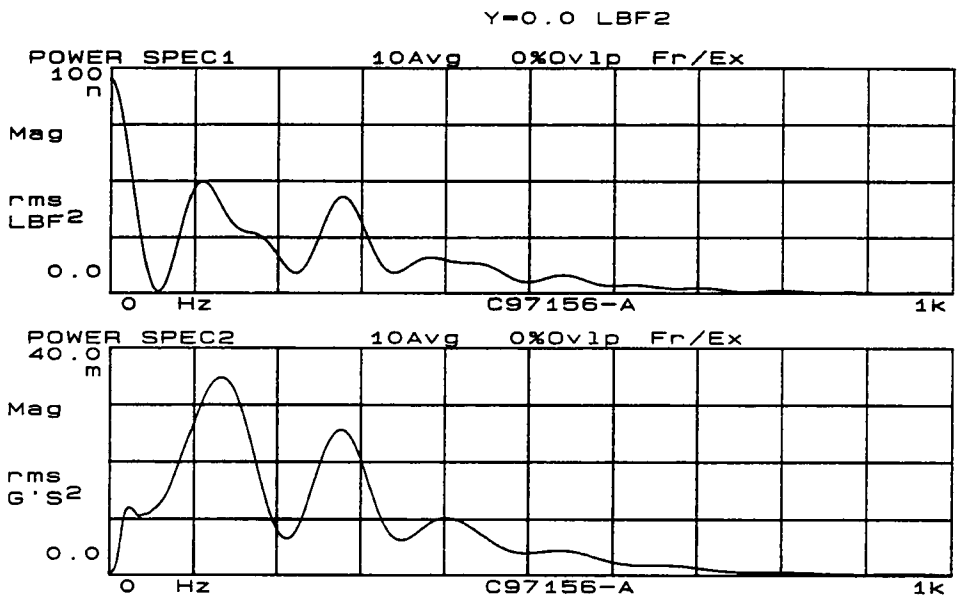


Figure 6-13. The power spectral curves from this ostectomized control specimen display the additional input and output energies frequently seen in the severely unstable bone specimens.

In power spectrum 1, instead of a clean input curve there are additional peaks indicating other sources of excitation. The impact hammer could have been in contact with the sample at separate points in time after the initial impact. These samples were very unstable and required a very light impact. In an attempt to keep from damaging the weak callus, the actual strike was not clean and crisp. In one case, only two strikes resulted in sufficient data for a calculated response.

The frequency range that can be induced by impact is limited by the stiffness of the contact surface and the mass of the hammer head according to (Ewins, 1984):

$$frequency = \sqrt{\frac{stiffness\ of\ contact\ surface}{hammer\ head\ mass}}$$

Adjustments can be made in the mass of the hammer head but these choices were limited and the softer head was already in use.

Low impact energy could have resulted in emphasizing the nonlinear behavior of the bone and its callus (Wasserman, 1998). Impacting the free end of the ostectomized bone generated more response, but in such weak systems this method could lead to excessive mass loading which could overdrive the system. The multiple peaks of the frequency response curve could have represented the excitation of double modes of response with one mode being linear and another nonlinear.

Different supporting conditions could have improved this test. For example, by supporting the free end as a pinned support, more input energy would have been possible and the deflection would have been emphasized at the callus site rather than at the free end of the bone.

In addition to better support of the sample, comparing two separate outputs could have helped to determine the linearity of the response. With an accelerometer distal and the other proximal to the callus, the parameters of natural frequency and damping from each of the accelerometers could have been compared. If no difference in these parameters occurred

between the two transducers, then the response would have been linear otherwise nonlinearity would explain the response.

One other possible adjustment would have been to vary the speed of the impact. The impact was done slowly in order to protect the soft callus but a slow impact could have increased the amount of time in contact with the surface and could have also resulted in "hammer bounce" where there were repeated contacts between the hammer and the surface of the bone.

The low energy of impact, severe instability, nonlinear behavior and possible mode shape alteration may have accounted for the multiple peaks seen in the output power spectrum. These peaks represented responses that were not accounted for solely by a single impact of the hammer. However, if hammer bounce had occurred, then these additional peaks in the output could have been the result.

As with the other groups a comparison between the behavior of the real and imaginary coefficients did correlate for resonant frequencies.

***Group 3***

Samples from group 3 had higher natural frequencies but similar frequency response curves as that of group 0. Coherence remained fairly good except in one case where it dropped below 0.5. The phenomenon noted in the input power spectrum of group 0 was not nearly as dramatic and was more consistent with the trial taped example. Again the

correlation between the real and imaginary coefficients was good. The callus in this group was palpably unstable.

*Group 6*

Tests from bone samples in group 6 were not significantly different from those in group 3. The natural frequencies were in the same range and the test curves were all similar. However, there was a significant difference between these two groups in the 3 - point bending Instron test. The lack of difference in natural frequencies may indicate that impact hammer testing was not sensitive enough to discriminate between the stiffness of a healing calluses separated by three weeks of somatotropin treatment.

*Group 12*

Frequency response curves from group 12 with the most advanced callus, had the highest natural frequencies of all the treatment groups. This was expected since increasing stiffness should result in an increase of the natural frequency by the following relation:

$$\omega_n = \sqrt{\frac{k}{m}}$$

These results paralleled the Instron data on the ultimate load to failure and stiffness as there was a statistically significant difference between the natural frequencies of the control group with a weak callus and the 12 week treatment group with a stable callus.

Also the frequency response curves in group 12 were similar in profile to that of an intact bone [Figure 6-14].

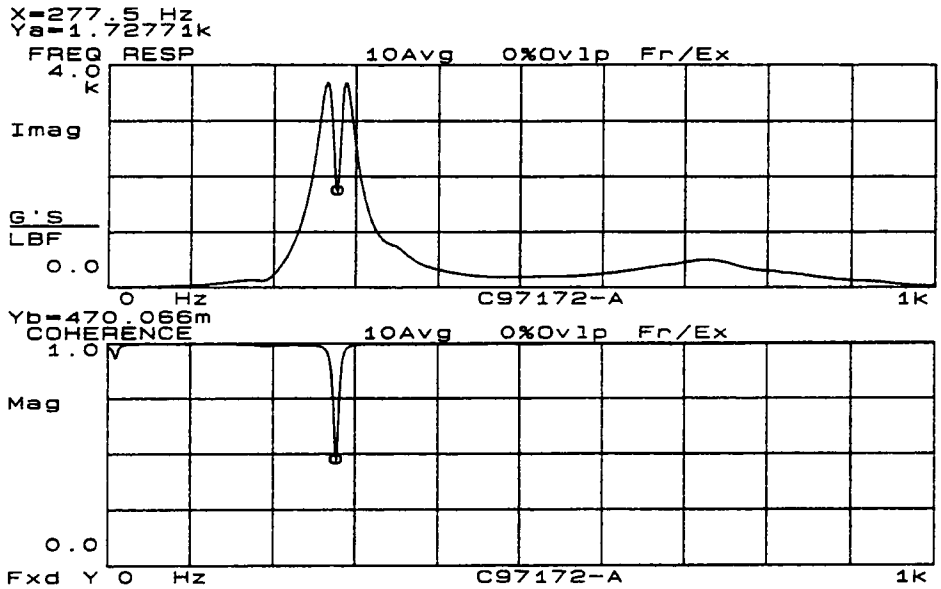


Figure 6-14. The frequency response curve from a 12 week treated ostectomy specimen with a stable callus displays the notched peak seen in some of the intact bone specimens.

The multiple frequency peaks past the initial peak seen in the previous three groups were not present in the 12 week group. Also the characteristic notching of the first resonant peak seen in the intact bone samples reappeared in this group. As in the intact bones this notch in the peak was associated with a drop in coherence.

The power spectral curves for group 12 were very similar to that of the intact bone. This observation led to the conclusion that the altered curves noted in the other groups were due to the instability of the healing callus and not to the testing setup or procedure.

### *Damping*

A second modal parameter, damping, was calculated from the frequency response data. These damping values were not statistically significant in discriminating among the various treatment groups.

The calculation of the percent of damping depended on the shape of the frequency response curve. The analyzer constructed a single degree of freedom fit to the curve in order to calculate the coefficients of the complex pole. Notched peaks or responses with excessive nonlinear behavior possibly influenced the damping calculation.

### *Impact Testing*

There are several methods of stimulating vibration in a test structure. Each of these methods have advantages and disadvantages. For this study an impact stimulus was selected. The advantage of impact testing was the speed of the test, as opposed to continuous stimulus testing where the calculation for the response takes a longer period of time.

The impact signal is transient and random. For nonlinear systems, a random stimulus is better than a harmonic stimulus; however, continuous random stimuli are more productive than transient stimuli in characterizing nonlinearity and removing distortion (Wasserman, 1984). However, in preliminary trials with a pinned-pinned support and continuous random stimuli, considerable problems were encountered. Repeatable results were not achieved and noise from the test support interfered with results.

Leakage occurs when the fast Fourier transform calculates a wave that is not periodic within the time record. Instead of clear frequency peaks there is a smearing of the information. This spreading of the energy throughout the frequency range is called leakage. With impact testing, leakage is minimized since all of the input signal is recorded within the finite test period. For continuous random waves that are not periodic within the time record, a mathematical adjustment can be made called "windowing". Windowing is more critical for continuous forcing functions that create continuous responses. For impact testing with a transient stimulus followed by a decaying response, leakage is minimal and windowing is not as critical. However, some windowing is beneficial to reduce the influence of noise. For impact testing a forcing function, which is essentially a unit step function, is multiplied with the impact function. This results in the maximizing of the data early in the period where the impact is occurring, and the minimizing of data at the end of the period where noise predominates the recorded signal. Along with this input window, a response window is also used. The response window is a decaying exponential function that when multiplied with the response function, the response data will be maximized early when the response is occurring and minimized late where again noise would tend to dominate the data.

Low signal to noise ratio is also a problem for impact testing. An effort can be made to reduce the production of noise from the impact by using a soft tip. In this study a plastic tip was used instead of a metal tip. The softer tip allows the hammer to be in contact with the test structure longer thereby reducing the opportunity for noise to obscure the hammer signal.

Another problem with the impact test is the difficulty in controlling the magnitude of the input signal and its frequency. Also the time of the impact affects the frequency range in that the longer the impact, the shorter the frequency range where some resonant frequencies could be missed.

Impact testing applies a large input signal over a short time period which tends to bring out nonlinearities within the system. For a system that is inherently nonlinear this input method is less desirable.

Due to the randomness of impact testing and the lack of control over the delivery of the input stimulus, single tests are not accurate in producing correct frequency responses. It becomes necessary to do several tests and average the data. With averaging, a method to evaluate the reliability of impact testing is the coherence function. The coherence function as a ratio of output to input assesses the reliability of a response being solely due to the input stimulus. The closer the value is to one, the more reliable the response.

# CHAPTER VII

# CONCLUSION

Statistical analysis confirmed that the natural frequency data obtained in this study appropriately discriminated between intact and ostectomized bone. In addition, the natural frequency data exhibited significant differences between the treatment groups indicating a level of sensitivity in the evaluation of the mechanical stability of healing fractures. Natural frequency results correlated well with the ultimate load to failure and stiffness data obtained from 3-point bending tests. This could have important implications in the possible application of vibrational testing to research and clinical orthopedics.

Statistical analysis did not confirm the significance of the damping data obtained in this test. Some trends in the performance of the damping data may be present; however, with the test protocol used herein, damping was not shown to be a reliable parameter for evaluation of fracture healing.

# CHAPTER VIII

# RECOMMENDATIONS FOR FUTURE STUDY

Several recommendations can be made regarding future study. Since damping was not a good discriminator, the excised bone study should be modified and repeated. This study could be enhanced by improving the supporting conditions. Severely unstable fractures need more support when placed under forced excitation. In addition to altering the support condition, the method of excitation could be changed. Continuous random excitation would diminish the nonlinearities that are inherent in the specimens studied.

The interpretation of the frequency response could be improved by expanding the protocol to include modal analysis. In this case several responses are recorded at different positions on the test sample. When analyzed the shape of the response can be displayed. Multiple modes can be investigated in this fashion. If the response in the unstable callus is due to the excitation of multiple modes, then modal analysis would be appropriate to verify this interpretation.

The next level of investigation should involve the inclusion of the soft tissue envelope and its effect on natural frequency and damping. Also, the evaluation of responses in different planes could enhance the reliability of vibrational testing in a clinical setting.

# REFERENCES

# REFERENCES


1. Ahl T, Kalen R. Effect of human growth hormone in the treatment of pseudoarthrosis. Opuscula Medica 1:26-28, 1979

2. Ashton IK, Dekel S. Fracture repair in the Snell dwarf mouse. Br J Exp Path 64:479-486, 1983

3. Bak B. Fracture healing and growth hormone. A biomechanical study in the rat. Dan Med Bull 40:519-536, 1993

4. Benirschke SK, Mirels H, Jones D, et al. The use of resonant frequency measurements for the noninvasive assessment of mechanical stiffness of the healing tibia. J Orthop Trauma 7:64-71, 1993

5. Best CH, Norman BT. The Physiological Basis of Medical Practice 8th ed, The Williams and Wilkins Co, Baltimore, Chapter 74: p 1492, 1966

6. Blevins RD. Formulas for Natural Frequency and Mode Shape, Krieger Publishing Co, Malabar FL, 1979

7. Brown SG, Kramer PC. Indirect (secondary) bone healing. Disease Mechanisms in Small Animal Surgery, 2nd ed, Bojrab MJ, Lea and Febiger, Phialdelphia, pp 671 - 677, 1993

8. Chao EYS, Aro HT. Biomechanics of fracture fixation. Basic Orthopedic Biomechanics, Van C. Mow and Wilson C. Hayes, Raven Press, Ltd, New York, 1991

9. Christensen AB, Ammitzboll F, Dyrbye C, et al. Assessment of tibial stiffness by vibration testing in situ -- I. Identification of mode shapes in different supporting conditions. J Biomech 19:53-60, 1986

10. Cornelissen P, Cornelissen M, Van-der-Perre G, et al. Assessment of tibial stiffness by vibration testing is situ -- II. Influence of soft tissue, joints and fibula. J Biomech 19:551-561, 1986

11. Cornelissen M, Cornelissen P, Van-der-Perre G, et al. Assessment of tibial stiffness by vibration testing in situ -- III. Sensitivity of different modes and interpretation of vibration measurements. J Biomech 20:333-342, 1987

12. De Arbogast. Personal Communication. Hewlett Packard Co., Everett, WA, 1998

13. Denis I, Pointillart A, Lieberherr M. Effects of growth hormone and insulin-like growth factor-I on the proliferation and differentiation of cultured pig bone cells and rat calvaria cells. Growth Regul 4:123-130, 1994

14. Ewins DJ. Modal Testing: Theory and Practice. Research Studies Press LTD, Taunton, Somerset, England, John Wiley and Sons Inc, New York, 1984

15. Farley JR, Baylink DJ. Biochemistry 21:3502, 1982

16. Fellinger M, Leitgeb N, Szyszkowitz R, et al. Early detection of delayed union in lower leg fractures using a computerized analysis of mechanical vibration reactions of bone for assessing the state of fracture healing. Arch Orthop Trauma Surg 113:93-96, 1994

17. Gere JM, Timoshenko SP. Mechanics of Materials, 2nd ed, PWS Engineering, Boston, 1984

18. Heckman JD, Boyan BD, Aufdemorte TB, et al. The use of bone morphogenic protein in the treatment of nonunion in a canine model. J Bone Joint Surg 73A:750-764, 1991

19. Herold HZ, Hurvitz A, Tadmore A. The effects of growth hormone on the healing experimental bone defects. Acta Orthop Scand 42:377-384, 1971

20. Hobatho MC, Darmana R, Pastor P, et al. Development of a three-dimensional finite element model of a human tibia using experimental modal analysis. J Biomech 24:371-383, 1991

21. Hsu JD, Robinson RA. Studies on the healing of long bone fractures in hereditary pituitary deficient mice. J Surg Res 9:535-536, 1969

22. Katz JL, Yoon HS. Indirect determination of the mechanical properties and mineral content of bone. Biomechanics of Physiological Mechanics, Injury Processes, Medical Procedures and Devices, Section IV, Chapter 3, 1975

23. Kohles SS, Cartee GS, Vanderby R Jr. Cortical elasticity in aging rats with and without growth hormone treatments. J Med Eng Tech 20:157-163, 1996

24. Laura PA, Rossie RE, Maurizi MJ. Dynamic analysis of a simplified bone model during the process of fracture healing. J Biomed Eng 12:157-160, 1990

25. Lowet G, Dayuan X, Van-der-Pere G. Study of the vibrational behavior of a healing tibia using finite element modelling. J Biomech 29:1003-1010, 1996

26. Lowet G, Van-Audekercke R, Van-der-Pere G, et al. The relation between resonant frequencies and torsional stiffness of long bones in vitro. Validation of a simple beam model. J Biomech 26:689-696, 1993

27. Markel MD, Bogdanske JJ. The effect of increasing gap width on localized densitometric changes within tibial ostectomies in a canine model. Calcif Tissue Int. 54:155-159, 1994

28. Markel MD, Chao EYS. Noninvasive monitoring techniques for quantitative description of callus mineral content and mechanical properties. Clin Orthop Rel Res 293:37-35, 1993

29. Millis DL, Wilkens BE, Daniel GB, et al. Radiographic, densitometric, and biomechanical effects of recombinant canine somatotropin in an unstable ostectomy gap model of bone healing in dogs. Vet Surg 27:85-93, 1998

30. Misol S, Samaan N, Ponseti IV. Growth hormone in delayed fracture union. Clin Orthop 74:206-208, 1971

31. Nikiforidis G, Bezerianos A, Dimarogonas A, et al. Monitoring of fracture healing by lateral and axial vibration analysis. J Biomech 23:232-330, 1990

32. Northmore-Ball MD, Wood MR, Meggitt BF. A biomechanical study of the effects of growth hormone in experimental fracture healing. J Bone Joint Surg 62B:391-396, 1980

33. Orne D. The in vivo driving point impedance of the human ulna: A viscoelastic beam model. J Biomech 7:249, 1974

34. Ricciardi L, Perissinotto A, Dabala M. Mechanical monitoring of fracture healing using ultrasound imaging. Clin Orthop Rel Res 292:71-76, 1993

35. Richards J. Stiffness in healing fractures. Crit Rev Biomed Eng 15:145-148, 1987

36. Shepanek LA. The effect of endocrine substances (ACTH and growth hormone) on experimental fractures. Surg Gynecol Obstet 96:200-204, 1953

37. Smith B. Personal Communication. Hewlett Packard Co., Everett, WA, 1998

38. Steele CR, Zhou L-J, Guido D, et al. Noninvasive determination of ulnar stiffness from mechanical response - In vivo comparison of stiffness and bone mineral content in humans. J Biomed Eng 110:87-88, 1988

39. Thomsen JJ. Modelling human tibia structural vibrations. J Biomech 23:215-228, 1990

40. Tylkowski CM, Wezeman FJ, Ray RD. Hormonal effects on the morphology of bone defect healing. Clin Orthop 115:274-285, 1976

41. Udupa KN, Gupta LP. The effect of growth hormone and thyroxine in healing of fracture. Ind J Med Res 53:623-628, 1965

42. Urist MR, DeLange RJ, Finerman AM. Bone cell differentiation and growth factors. Science 220:680-686, 1983

43. Van-der-Perre G, Van-Audekercke R, Martens M, et al. Identification of in-vivo vibrations modes of human tibiae by modal analysis. J Biomech Eng 105:244-248, 1983

44. Volpon JB. Nonunion using a canine model. Arch Orthop Trauma Surg 113:312-317, 1994

45. Wasserman JF. Personal Communication, 1998

46. Wasserman JF. Modern Methods in Experimental Vibrations, University of TN, 1984

47. Wilkens BE, Millis DL, Daniel GB, et al. Metabolic and histologic effects of recombinant canine somatotropin on bone healing in dogs, using an unstable ostectomy gap model. Am J Vet Res 57:1395-1401, 1996

48. Wray JB, Goldstein J. The effect of the pituitary gland and growth hormone upon the strength of the healing fracture in the rat. J Bone Joint Surg 48A:815-816, 1966

49. Zadek RE, Robinson RA. The effect of growth hormone on experimental long-bone defects. J Bone Joint Surg 43A:1261, 1961

# BIBLIOGRAPHY

# BIBLIOGRAPHY


1. Gere JM, Timoshenko SP. Mechanics of Materials, 2nd ed, PWS Engineering, Boston, 1984

2. Hewlett Packard. The Fundamentals of Signal Analysis. Application Note 243

3. Hewlett Packard. 3562 Dynamic Signal Analyzer Operating Instructions

4. Thomson WT. Theory of Vibration with Applications, 3rd ed, Prentice Hall, New Jersey, 1988

5. Wasserman JF. Modern Methods in Experimental Vibrations, University of TN, 1984

# VITA

Joseph Paul Weigel was born in Cheyenne, Wyoming on September 30, 1947. He moved to Aurora, Colorado and attended parochial elementary and secondary schools. Following graduation from Machebeuf High School, he attended Colorado State University in Fort Collins, Colorado. He graduated in 1969 with a Bachelor of Science in Biology and in 1972 with a Doctor of Veterinary Medicine. Following graduation he was an intern and junior staff veterinarian at the Angell Memorial Animal Hospital in Boston, Massachusetts. In 1976 he completed a surgical residency program at the University of California, Veterinary Teaching Hospital. Following the residency program, he accepted a faculty position in the Department of Urban Practice, College of Veterinary Medicine, University of Tennessee. In 1983, he successfully completed the certification requirements for membership in the American College of Veterinary Surgeons. His professional experience has focused on small animal orthopedic surgery. Out of this interest, he pursued additional education in solid mechanics which led to this presentation for a Master of Science in Engineering Science, 1998.